UNIVERSITY OF OKLAHOMA

GRADUATE COLLEGE

PALEOMAGNETIC DATING OF BURIAL DIAGENESIS IN MISSISSIPPIAN CARBONATES, UTAH

A THESIS

SUBMITTED TO THE GRADUATE FACULTY

in partial fulfillment of the requirements for the

degree of

MASTER OF SCIENCE

By

ANGELA M. BLUMSTEIN
Norman, Oklahoma
2003

PALEOMAGNETIC DATING OF BURIAL DIAGENESIS IN MISSISSIPPIAN CARBONATES, UTAH

A THESIS APPROVED FOR THE
SCHOOL OF GEOLOGY AND GEOPHYSICS

BY

[redacted]

ACKNOWLEDGEMENTS

I would like to thank my advisor, Dr. Doug Elmore, for his continuous support and enthusiasm, and for giving me the opportunity to work on this project. My appreciation goes to Dr. Mike Engel for his assistance in the field as well as in the remainder of the project. I would also like to express my appreciation to Dr. Kevin Smart for his assistance with this project.

I would like to thank my husband, Raleigh, for his understanding and support while I was attending college and working on this project. His friendship, encouragement, and patience have been a constant source of motivation in college as well as in every other aspect of my life.

I also want to thank my parents, Dave and Jo Miller, for their encouragement during this project as well as their constant support and guidance throughout my life. My greatest appreciation goes to all of my family and friends for their moral support and to Marilyn Trollinger for encouraging me to take a geology class.

My gratitude goes to Dr. Michael Lewchuk for his thoughtful discussions and ideas that aided in this project. I also extend my thanks to Eric Cox and the under-graduate students for helping me in the paleomagnetism laboratory.

Funding for this project was provided by DOE grant DE-FG03-96ER14643 and a research grant from the American Association of Petroleum Geologists Foundation.

TABLE OF CONTENTS

LIST OF TABLES

LIST OF FIGURES

ABSTRACT

The objective of this study is to test models for the origin of widespread remagnetizations in the Mississippian Deseret Limestone. The Delle Phosphatic Member of the Deseret Limestone is a source rock for hydrocarbons in other units in Utah and entered the oil window in the Early Cretaceous during the Sevier orogeny based on modeling studies. Paleomagnetic results from the Deseret Limestone and the stratigraphically equivalent Chainman Shale in central and western Utah indicate that the unit contains two dual polarity ancient magnetizations, interpreted to be chemical remanent magnetizations (CRMs) based on low burial temperatures. The demagnetization characteristics and rock magnetic studies indicate that the CRMs reside in magnetite. Three fold tests from western Utah indicate the presence of a pre-folding Triassic to Jurassic CRM. Geochemical ($^{87}Sr/^{86}Sr$, $\delta^{13}C$, and $\delta^{18}O$) and petrographic analyses suggest that these rocks are unaltered. The age of the CRM is just prior to the modeled time for organic matter maturation in the unit. Therefore, this CRM is interpreted to be the result of burial diagenesis, such as an early stage of organic matter maturation within the source rock or clay alteration. A second younger CRM in western and central Utah is post-folding based on a regional fold test. This CRM is Late Cretaceous to Early Tertiary in age and the timing overlaps with the oil window based on the thermal modeling. These results are also consistent with a connection between organic matter maturation and remagnetization, and the geochemical ($^{87}Sr/^{86}Sr$, $\delta^{13}C$, and $\delta^{18}O$) and petrographic results from rocks with this component show no evidence for alteration by externally derived fluids. The results of this study support the hypothesis that widespread burial diagenetic processes are associated with pervasive CRMs. In addition, this study

indicates that paleomagnetism can be used to determine the timing of burial diagenetic processes, which can benefit hydrocarbon exploration efforts.

INTRODUCTION

The timing of burial diagenetic processes is an important issue in understanding the history of a formation both stratigraphically and structurally. The timing of these processes is essential in hydrocarbon exploration to understand the age relationship between source rock maturation, hydrocarbon migration, and trap formation. Maturation of organic matter is currently dated indirectly by combining data such as conodont alteration, vitrinite reflectance, and burial curves. Therefore, the ability to date organic matter maturation more directly would aid in exploration efforts.

The objective of this study is to test models for the origin of widespread remagnetizations in the Mississippian Deseret Limestone, and to specifically test a paleomagnetic method for dating burial diagenetic processes such as maturation of organic matter. Previous studies have provided evidence that pervasive chemical remanent magnetizations (CRMs) can be associated with burial diagenetic processes such as organic matter maturation (Plaster-Kirk et al., 1995; Banerjee et al., 1997) or clay diagenesis (e.g., Katz et al., 2000). Additional studies are needed, however, to fully validate the dating approach. Testing the origin of pervasive CRMs will also provide useful information because the origin of such magnetizations has been controversial. Whereas some pervasive CRMs are interpreted to be related to burial diagenetic processes, fluids activated as a result of orogenic activity (e.g., Oliver, 1992) are also a commonly hypothesized agent of remagnetization. As a consequence, the origin of such pervasive CRMs is unresolved.

The Delle Phosphatic Member of the Deseret Limestone is a source rock for hydrocarbons in other units in Utah. Based on modeling studies, it entered the oil

window in the Early Cretaceous during the Sevier orogeny (Huntoon et al., 1999). To test for a connection between remagnetization and maturation of organic matter, samples were collected for three fold tests in western Utah and a regional fold test between central and western Utah to constrain the timing of the magnetizations. The pole positions were compared to the apparent polar wander path to establish the age of the CRMs and the age was compared to the depth versus burial curve for the Deseret Limestone (Huntoon et al., 1999) to test for a relationship between the CRM and maturation of organic matter. Geochemical ($^{87}Sr/^{86}Sr$, $\delta^{13}C$, and $\delta^{18}O$) and petrographic analyses were also conducted to determine if the samples have undergone any alteration by orogenic or hydrothermal fluids.

GEOLOGIC SETTING

The Mississippian Deseret Limestone and the laterally equivalent Chainman Shale were deposited in the Deseret Basin of western and central Utah (Figure 1). The Deseret Basin is a foreland basin that formed in response to the Antler Orogeny. The major thrust movement associated with the Antler Orogeny occurred in Late Devonian and Early Mississippian time in central and eastern Nevada (Sandberg et al., 1980). The sediments of the Deseret Basin were deposited east of the Antler Highlands at the paleoequator during Mississippian time (Sandberg and Gutschick, 1984). Samples of the Deseret Limestone and Chainman Shale were collected throughout western and central Utah in the Confusion Range (CR), Mountain Home Range (MHR), Pavant Range (PR), Oquirrh Mountains (OM), Johnson Pass (JNP), and Stansbury Mountains (SM) (Figure 1).

The lithology of the Delle rocks and the lower members of the associated Deseret Limestone and Chainman Shale consist mainly of interbedded claystone, mudstone, shale, micritic limestone, phosphorite, and chert. The rocks generally have a dark gray color, fine texture, thin bedding, and are weakly resistant to weathering (Sandberg and Gutschick, 1984). For this study, the thin micritic limestones, which were interbedded with thick shales, were the primary lithology sampled.

The depositional environment of the Deseret Limestone and its equivalent sediments in the Deseret Basin has been the subject of debate. One model (Sandberg and Gutschick, 1980; 1984) proposes that the Osagean to Meramecian Delle Phosphatic Member is the basal member of the Deseret Limestone in central Utah and the Chainman Shale in western Utah (Figure 2). It was deposited in a regionally-extensive, moderately

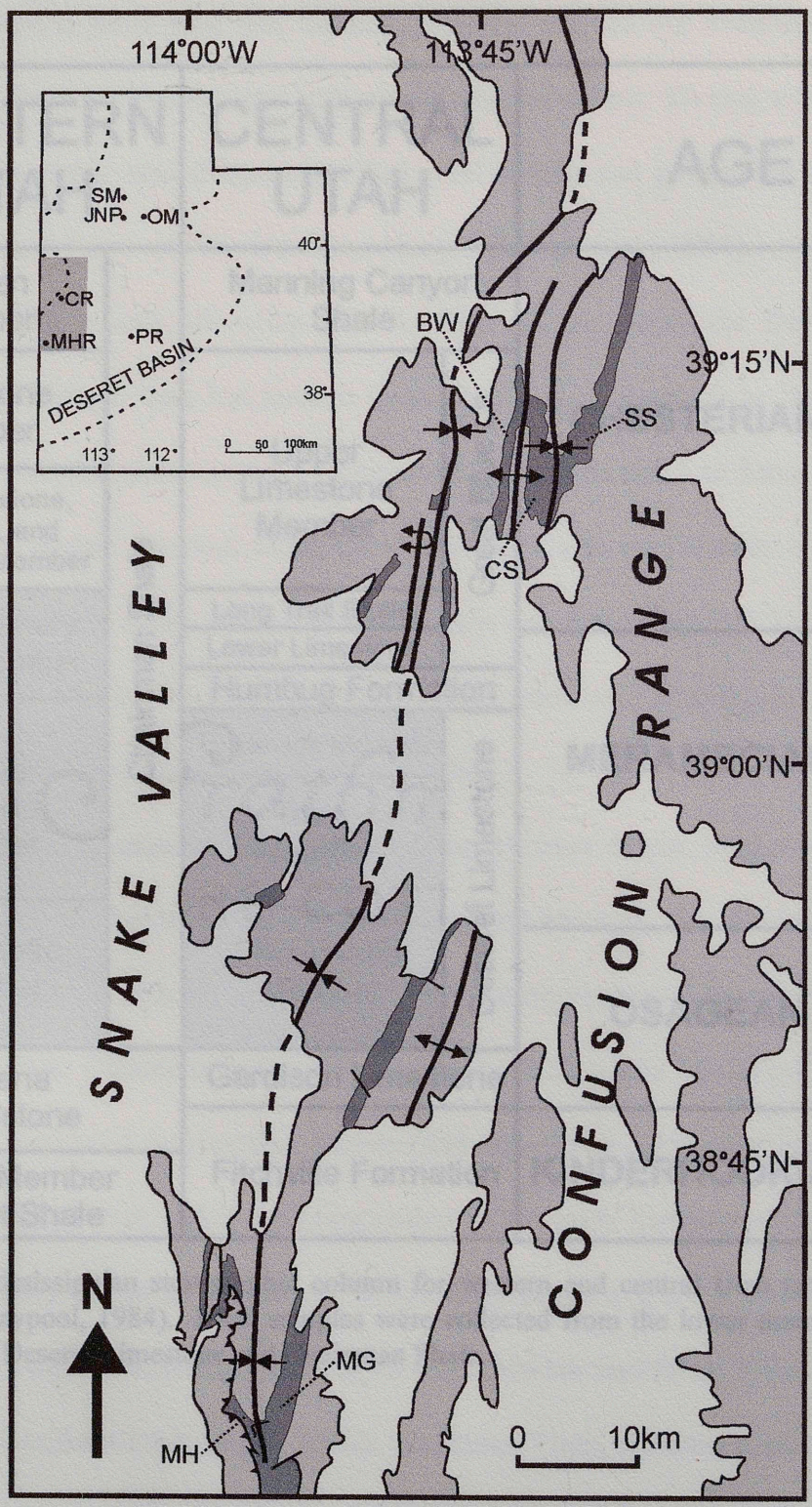

Figure 1: Location of study area in Utah. Inset map shows the location of the Deseret Basin (Lat: 37-44 °N, Lon: 111-116°W) and the sampling locations in Utah; Conger Range (CR), Mountain Home Range (MHR), Pavant Range (PR), Stansbury Mountains (SM), Johnson Pass (JNP), Oquirrh Mountains (OM) (modified from Sandberg and Gutschick, 1984). The sampled limbs of the anticline-syncline couplet in the Confusion Range (BW, CS, SS) and the syncline in the Mountain Home Range (MH, MG) are labeled. The light gray shading represents the mountain ranges and the dark gray shading represents the Chainman Shale.

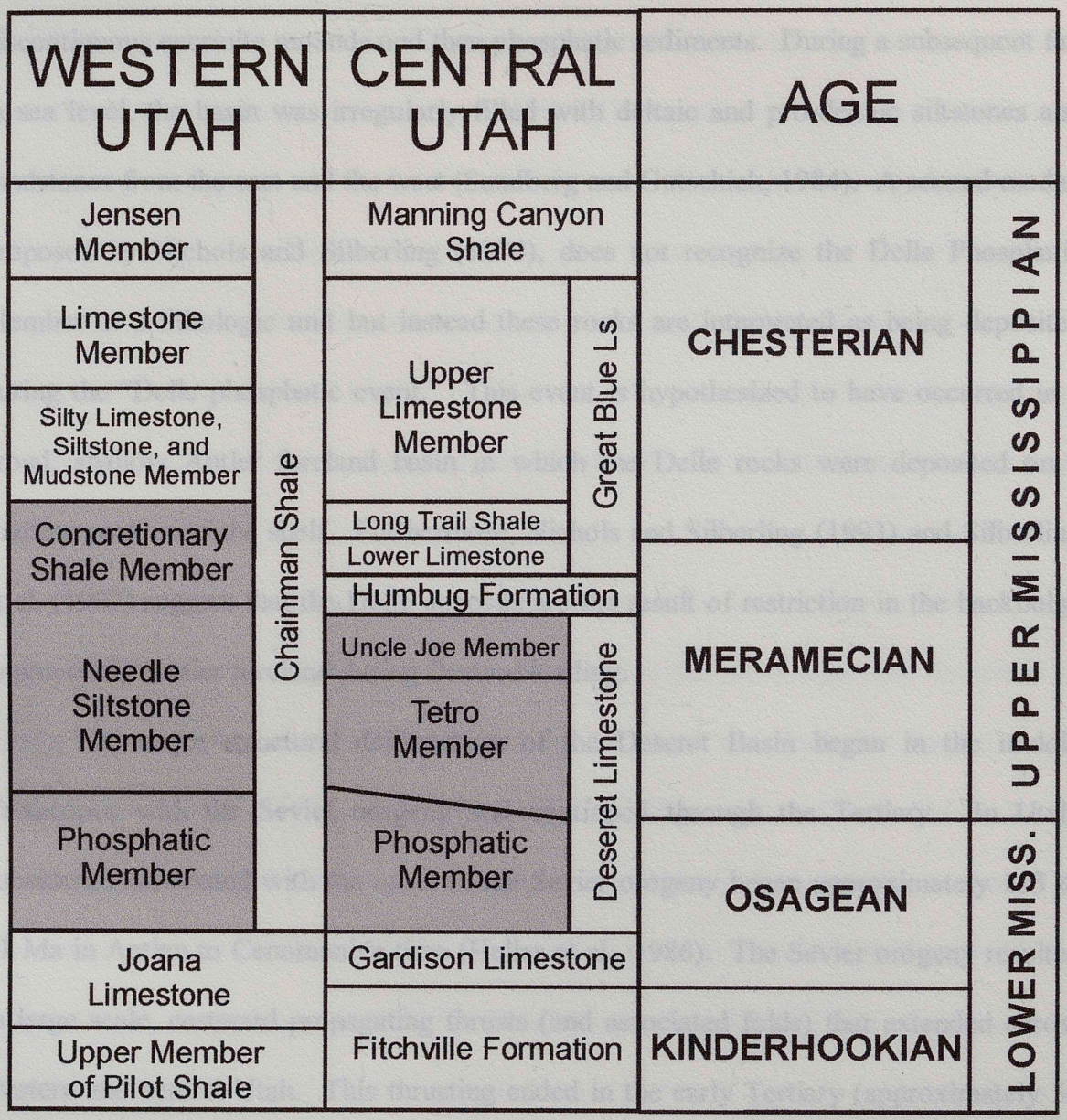

Figure 2: Mississippian stratigraphic column for western and central Utah (modified from Poole and Claypool, 1984). Most samples were collected from the lower members (shaded above) of the Deseret Limestone and Chainman Shale.

deep (300+ meters) basin that was initially sediment starved but eventually filled with discontinuous encrinite mounds and then phosphatic sediments. During a subsequent fall in sea level, the basin was irregularly filled with deltaic and pro-deltaic siltstones and sandstones from the east and the west (Sandberg and Gutschick, 1984). A second model, proposed by Nichols and Silberling (1990), does not recognize the Delle Phosphatic Member as a lithologic unit but instead these rocks are interpreted as being deposited during the "Delle phosphatic event." This event is hypothesized to have occurred in a broad, shallow Antler foreland basin in which the Delle rocks were deposited on a shallow portion of the shelf. Furthermore, Nichols and Silberling (1993) and Silberling et al. (1997) suggest that the Delle deposits are the result of restriction in the backbulge region of the Antler foreland during flexural loading.

The major structural deformation of the Deseret Basin began in the middle Cretaceous with the Sevier orogeny and continued through the Tertiary. In Utah, subsidence associated with the onset of the Sevier orogeny began approximately 113 to 91 Ma in Aptian to Cenomanian time (Heller et al., 1986). The Sevier orogeny resulted in large scale, eastward propagating thrusts (and associated folds) that extended across western and central Utah. This thrusting ended in the early Tertiary (approximately 50 Ma) and extension began in the former Sevier orogenic belt about 49 Ma (Bird, 1998). The Laramide orogeny lasted from about 75 to 35 Ma but had little, if any, effect in the study areas of western Utah (Bird, 1998). In central Utah, structures are dominated by Sevier age thrusts but are superimposed by Laramide uplift and faulting (Baer et al., 1982). In the late Tertiary and early Quaternary, north-south trending normal faults formed the Basin and Range province seen today throughout Utah (Beratan, 1996).

In this study, asymmetric Sevier age folds were sampled. The anticline and syncline sampled in the Confusion Range are plunging to the south approximately 3° and the west-dipping limbs have the steepest dips. The syncline sampled in the Mountain Home Range plunges to the northwest approximately 18° and the east-dipping limb has the steepest dip. Extensional features have also been documented in the Confusion Range that are Eocene to Oligocene in age (Nichols et al., 2002). Nichols et al. (2002) have noted down-to-the-west tilt (25° or less) along the west side of the Confusion Range and believe that there are modest down-to-the-east dips in the Mountain Home Range (Silberling, 2002).

The source rock potential is also an important issue with respect to the proposed objective of this study. The Delle Phosphatic Member has previously been described by Huntoon et al. (1999) as the most likely source rock for the Giant Tar Sand Triangle accumulation in eastern Utah. According to the modeling conducted in the Pavant Range by Huntoon et al. (1999), the Delle Phosphatic Member reached maturity at about 161 Ma and overmaturity at about 88 Ma. The peak generation in the Pavant Range ($\%R_o$ = 1.0) occurred at approximately 93 Ma (Huntoon et al., 1999). The Delle Phosphatic Member contains 3 to 8 wt. % total organic carbon (TOC) of types II and III kerogens in outcrop samples (Poole and Claypool, 1984) and higher TOC values (6.7-13.3 wt. %) were obtained from core samples (Morris and Lovering, 1961). The lower three members of the Chainman Shale (Figure 2) have a relatively high organic-carbon content, with an average of 1.8 wt. % (Sandberg et al., 1980). The sampling locations in the Confusion Range, Mountain Home Range, and Pavant Range have conodont color-alteration index (CAI) values of 1.5 or 2, indicating that these rocks have never been

heated to temperatures higher than 90°-140°C (Sandberg et al., 1980). The Oquirrh Mountains have a CAI value of 5 (Sandberg et al., 1980) indicating that these rocks have been heated to temperatures greater than 300°C.

METHODS

Samples for paleomagnetic and geochemical study were collected from the Mississippian Deseret Limestone and Chainman Shale at 9 locations in western and central Utah (Figure 1). The micritic limestones of the Delle Phosphatic Member were the primary lithology sampled. However, some samples were also taken from the overlying members (Figure 2). In western Utah, the Chainman Shale was sampled on three limbs of an anticline-syncline couplet in the Confusion Range (Figure 1). Samples were also collected on both limbs of a syncline in Mountain Home Range approximately 50 km south of the anticline-syncline couplet (Figure 1). In central Utah, samples were collected in the Oquirrh Mountains, Johnson Pass, and the Pavant Range as well as on a syncline in the Stansbury Mountains (Figure 1).

A gasoline powered drill was used to core the samples in the field which, were oriented with a Brunton compass and inclinometer. In the lab, each core was cut to standard lengths (approximately 2.2 cm) and paleomagnetic data was obtained using a 2G Enterprises cryogenic magnetometer with DC squids located in a magnetically shielded room. The natural remanent magnetizations (NRMs) were determined and the specimens were thermally demagnetized in a magnetically shielded Schonstedt TSD-1 or an ASC thermal demagnetizer oven at the following temperatures: 100, 150, 200, 250, 275, 300, 320, 340, 360, 380, 400, 420, 440, 460, 480, 500, 520, 540, 560, 580, 600, 625, 650, 675, and 700°C. Alternating field (AF) demagnetization of the NRMs up to 120mT displayed curved paths and did not clearly resolve the remanent components. As a result, it was not used to derive directional information.

The demagnetization data were plotted in Zijderveld (1967) diagrams and principal component analysis (Kirschvink, 1980) was used to determine magnetic directions. Most specimens had components with mean angular deviations (MAD) of less than 10°, however, some components had deviations up to 15°. The mean directions were calculated using Fisher (1953) statistics and the Super-IAPD99 software. The Watson and Enkin (1993) fold test was conducted on the data from the folds in the Confusion Range, Mountain Home Range, and Stansbury Mountains. The results from the fold tests were used to determine poles that were plotted on a North American apparent polar wander path constructed by Van der Voo (1993).

Low temperature analysis, AF demagnetization, and isothermal remanent magnetization (IRM) acquisition were also conducted to determine the magnetic mineralogy of the specimens. Low temperature analysis was conducted on selected specimens that were submerged in liquid nitrogen and subjected to temperatures below -155°C. The specimens were then warmed to room temperature before undergoing thermal demagnetization. The AF demagnetization was conducted using a 2G Automated Degaussing System on a set of specimens up to 120mT and an impulse magnetizer was then used to acquire an IRM up to 2500mT. Next, the specimens underwent AF demagnetization for a second time up to 120mT and then a series of backfield measurements were taken using the impulse magnetizer. Finally the specimens were subjected to three perpendicular IRMs at 120mT, 500mT, and 2500mT and thermally demagnetized to determine the triaxial IRM decay (Lowrie, 1990).

Microscopic analysis was performed on polished thin sections using both reflected and transmitted light to determine the mineralogy. The rocks were classified

using Dunham's (1962) classification scheme for limestones and diagenetic features were noted.

The carbon and oxygen isotopic signatures were obtained for 35 micritic limestones from different sampling sites. The samples were prepared by sealed tube reaction of the carbonate with 100% phosphoric acid (H_3PO_4) at 50°C for two hours (McCrea, 1950; Swart et al., 1991). The resulting gas was then analyzed for both carbon and oxygen isotope abundances and reported in delta notation (δ) in parts per thousand (‰) relative to the PeeDee Belemnite (PDB) standard. The stable oxygen isotope values were corrected to 25°C after Swart et al. (1991).

Strontium isotope analysis was performed on 12 micritic limestone samples at the University of Texas at Austin following the methods described in Gao et al. (1992). Standard SRM 987 was routinely analyzed during this study and yielded 0.710266 ± 0.000007 (1σ = 0.00001, n = 3). The $^{87}Sr/^{87}Sr$ ratios of the samples were normalized relative to NBS 987 = 0.71014. The $^{87}Sr/^{86}Sr$ ratios were then compared to the coeval seawater values for Mississippian (Osagean to Meramecian) age limestones as determined by Denison et al. (1994).

RESULTS AND INTERPRETATIONS

Paleomagnetism

Thermal demagnetization of specimens resulted in the identification of three components (Figure 3a). A component with northerly declinations and steep down inclinations is present in most specimens and it is removed at low temperatures (Figure 3a). This component is interpreted as a modern viscous remanent magnetization (VRM). Component 1, with southerly declinations and shallow up inclinations, is present at 7 sample locations (Figures 3a and 3b). Component 2 is present at 3 locations and has northwesterly declinations and moderate down inclinations (Figures 3a and 3c). Antipodal directions for both components are found in specimens at some sites (Figures 3d and 3e).

Component 1 is present at 16 of the sites sampled in the Confusion Range and Mountain Home Range (Table 1a). This component is typically removed from 275°-500°C (Figure 3b). However, in specimens that contain components 1 and 2, component 1 decays to temperatures up to 560°C (Figure 3a). Within the sites, the specimen directions are well grouped (Figure 4; Table 1a).

Specimens from site CS3 have a component with northerly declinations and shallow down inclinations (Figures 3d and 4) that decays between 380 and 420°C. A reversal test (McFadden and Lowes, 1981) was performed on the specimen directions from sites CS1 and CS3 and the results show that the directions are not distinct. The direction at site CS3 is interpreted as an antipode to the reversed directions of component 1.

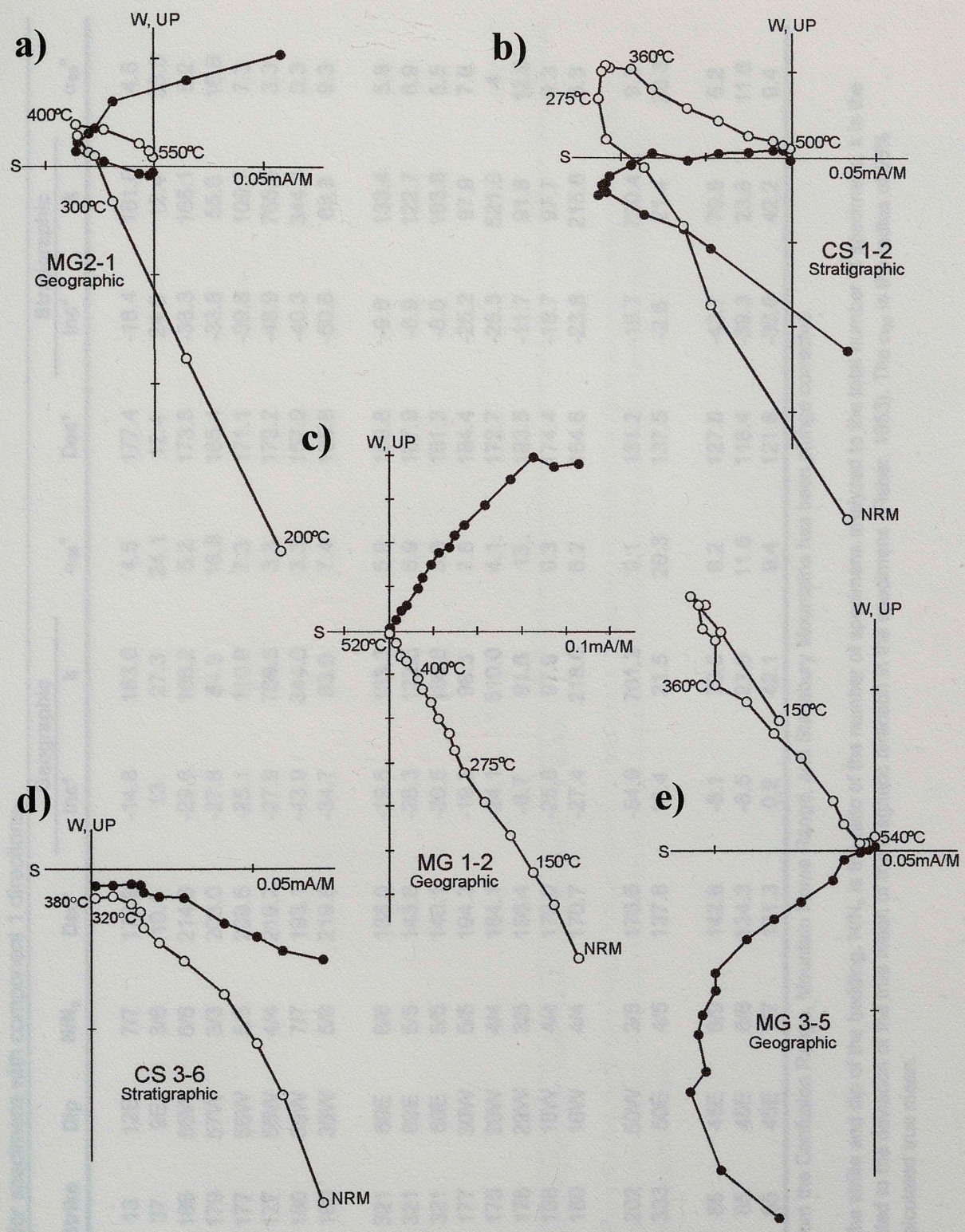

Figure 3: Representative orthogonal projections of thermal demagnetization data from different locations in Utah showing the remanent components: a) VRM (200-300°C), component 1 (300-400°C) and component 2 (400-550°C), NRM removed because of scale, b) component 1 (360-500°C), c) component 2 (275-520°C), d) component 1 antipode (320-380°C), and e) component 2 antipode (360-540°C), NRM removed because of scale. The horizontal component is represented by the closed circles and the vertical component is represented by the open circles.

Table1a: Site means for specimens with component 1 directions.

Location/Site	Strike	Dip	N/N_o	Geographic Dec°	Geographic Inc°	Geographic k	Geographic α_{95}°	Stratigraphic Dec°	Stratigraphic Inc°	Stratigraphic k	Stratigraphic α_{95}°
Confusion Range											
CS 1	13	12E	7/7	173.9	-14.8	183.0	4.5	177.4	-18.4	181.0	4.5
CS 3*	37	9E	3/6	10.1	13	27.3	24.1	12.4	24.8	12.4	36.5
BW 1	186	55W	6/6	214.3	-29.3	166.2	5.2	173.8	-38.3	168.1	5.2
BW 2	179	57W	3/3	203.0	-27.8	54.9	16.8	165.4	-33.8	55.0	16.8
BW 3	177	56W	5/5	209.5	-25.1	110.0	7.3	171.1	-39.8	109.7	7.3
BW 4	177	56W	4/4	219.2	-27.9	769.5	3.3	172.2	-48.9	766.6	3.3
SS 2	180	38W	7/7	193.1	-43.9	344.0	3.3	157.0	-40.3	344.3	3.3
SS 3	180	38W	5/6	219.8	-34.7	83.0	7.4	185.8	-50.6	68.3	9.3
Mountain Home Pass											
MH 4	321	69E	6/6	138.0	-19.6	133.3	5.8	159.8	-9.6	133.4	5.8
MH 5	321	69E	5/5	143.6	-26.3	122.5	6.9	167.9	-6.9	122.7	6.9
MH 6	321	69E	5/5	140.1	-20.5	189.8	5.6	161.3	-8.0	193.6	5.5
MG 2	177	30W	5/5	194.3	-19.2	98.3	7.8	184.4	-25.2	97.9	7.8
MG 5	175	29W	4/4	184.1	-24.1	510.0	4.1	172.7	-25.3	521.0	4
MG 7	178	29W	3/5	186.4	-8.7	91.6	13	183.5	-11.7	91.8	12.9
MG 9	198	18W	4/4	179.0	-25.6	97.9	9.3	174.4	-18.7	97.7	9.3
MG 10	180	16W	4/4	170.7	-27.4	218.0	6.2	164.6	-23.8	215.6	6.3
Stansbury Mountains											
SM2	202	50W	2/5	176.5	-54.9	761.3	9.1	151.2	-19.7	730.4	9.3
SM4	333	50E	4/5	137.8	13.4	21.5	20.3	137.5	-2.6	21.4	20.3
Johnson Pass											
JNP 1	85	45E	8/9	142.6	-8.1	79.8	6.2	127.8	-43.7	79.8	6.2
JNP 2	85	45E	8/8	134.3	-8.5	23.8	11.6	118.4	-39.3	23.8	11.6
JNP 3	85	45E	7/7	131.3	0.2	42.1	9.4	121.6	-30.6	42.2	9.4

The stratigraphic data from the Confusion Range, Mountain Home Range, and Stansbury Mountains has been plunge corrected.

*Component 1 anitpode

Note: Stike and dip are the strike and dip of the bedding, N/N_o is the ratio of the number of specimens analyzed to the total number of specimens, k is the precision parameter related to the deviation of the true mean of the magnetic direction in the specimens (Fisher, 1953). The α_{95} is the radius of 95% probability around the calculated true mean.

Table 1b: Site means for specimens with component 2 directions.

Location/Site	Strike	Dip	N/N_o	Geographic Dec°	Geographic Inc°	Geographic k	Geographic α_{95}°	Stratigraphic Dec°	Stratigraphic Inc°	Stratigraphic k	Stratigraphic α_{95}°
Mountain Home Pass											
MG1	167	34W	5/5	305.8	45.1	470.0	3.5	293.1	19.1	469.0	3.5
MG2	177	30W	3/5	314.8	57.8	108.2	11.9	297.8	33.6	107.4	12.0
MG3*	174	32W	4/5	124.8	-38.3	39.9	14.7	118.0	-12.2	39.9	14.7
MG4A	170	37W	4/4	8.6	47.7	59.1	12	329.2	46.0	59.0	12.1
MG5	175	29W	2/4	344.6	61.4	12.5	78.1	310.4	46.6	12.5	78.0
MG6	175	30W	4/4	248.7	68.5	56.1	12.4	259.7	39.0	55.8	12.4
MG7	178	29W	3/5	286.2	67.5	23.1	26.3	279.3	39.2	23.0	26.3
MG9	198	18W	2/4	319.6	41.6	42.4	39.4	316.0	25.8	42.7	39.2
Pavant Range											
CF1	8	33E	2/3	353.4	67.1	76.0	29.0	56.1	55.7	76.0	29.0
CF2	8	33E	2/3	58.7	71.0	179.0	18.7	82.2	41.0	178.0	18.8
CF3	8	33E	5/5	14.0	68.2	208.0	5.3	63.5	49.2	209.0	5.3
Oquirrh Mountains											
OPR1*	145	40W	9/10	126.5	-42.1	13.6	14.5	104.0	-21.2	13.6	14.5
OPR2*	145	40W	5/7	116.7	-32.5	29.9	14.2	103.7	-8.9	29.7	14.3

The stratigraphic data from the Mountain Home Range has been plunge corrected.

*Component 2 antipode

Note: Strike and dip are the strike and dip of the bedding, N/N_o is the ratio of the number of specimens analyzed to the total number of specimens, k is the precision parameter related to the deviation of the true mean of the magnetic direction in the specimens (Fisher, 1953). The α_{95} is the radius of 95% probability around the calculated true mean.

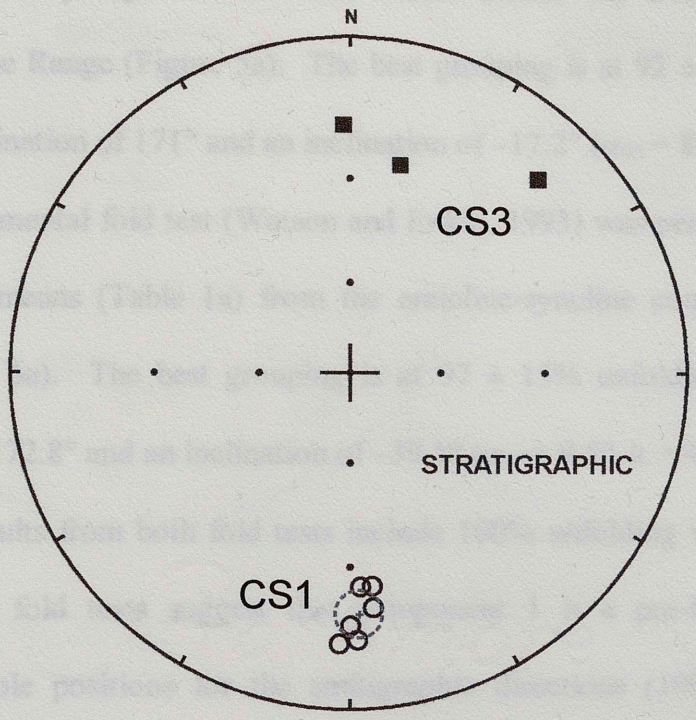

Figure 4: Equal area projections for component 1 showing a typical grouping of specimen directions (site CS1, circles) and specimen directions of the antipode to component 1 (site CS3, squares). The open symbols represent negative inclinations and closed symbols represent positive inclinations.

Fold tests were conducted on the component 1 data from the Mountain Home Range and Confusion Range. The Watson and Enkin (1993) incremental fold test was conducted on the plunge-corrected site means (Table 1a) from the syncline in the Mountain Home Range (Figure 5a). The best grouping is at 92 ± 9% unfolding (Figure 5b) with a declination of 171° and an inclination of –17.2° (α_{95} = 8.3°, k = 46.1; Table 2). A second incremental fold test (Watson and Enkin, 1993) was performed on the plunge-corrected site means (Table 1a) from the anticline-syncline couplet in the Confusion Range (Figure 6a). The best grouping is at 97 ± 15% unfolding (Figure 6b) with a declination of 172.8° and an inclination of –39.1° (α_{95} = 9.5°, k = 41.1; Table 2).

The results from both fold tests include 100% unfolding within the error limits. Therefore, the fold tests suggest that component 1 is a pre-folding magnetization. Plotting the pole positions for the stratigraphic directions (100% unfolding) on the apparent polar wander path (APWP) for North America (Van der Voo, 1993) indicates that component 1 is Late Triassic to Early Jurassic in age (Figure 7).

The Tertiary tilt observed in the Confusion Range and Mountain Home Range (Nichols et al., 2002) was accounted for by correcting the geographic directions for the maximum tilt, correcting for the plunge, and then performing the fold test. The tilt correction does not significantly change the grouping of the site means. The tilt corrected pole positions were compared with the uncorrected poles on the APWP. Removing the maximum of 25 degrees of westerly tilt in the Confusion Range gives a new pole position of 58.7°N, 118.4°E which is close to the uncorrected pole. Removing 25 degrees of easterly tilt in the Mountain Home Range gives a pole position of 58.8°N, 59.2°E which does not significantly change the inferred age of the component. Since the declinations

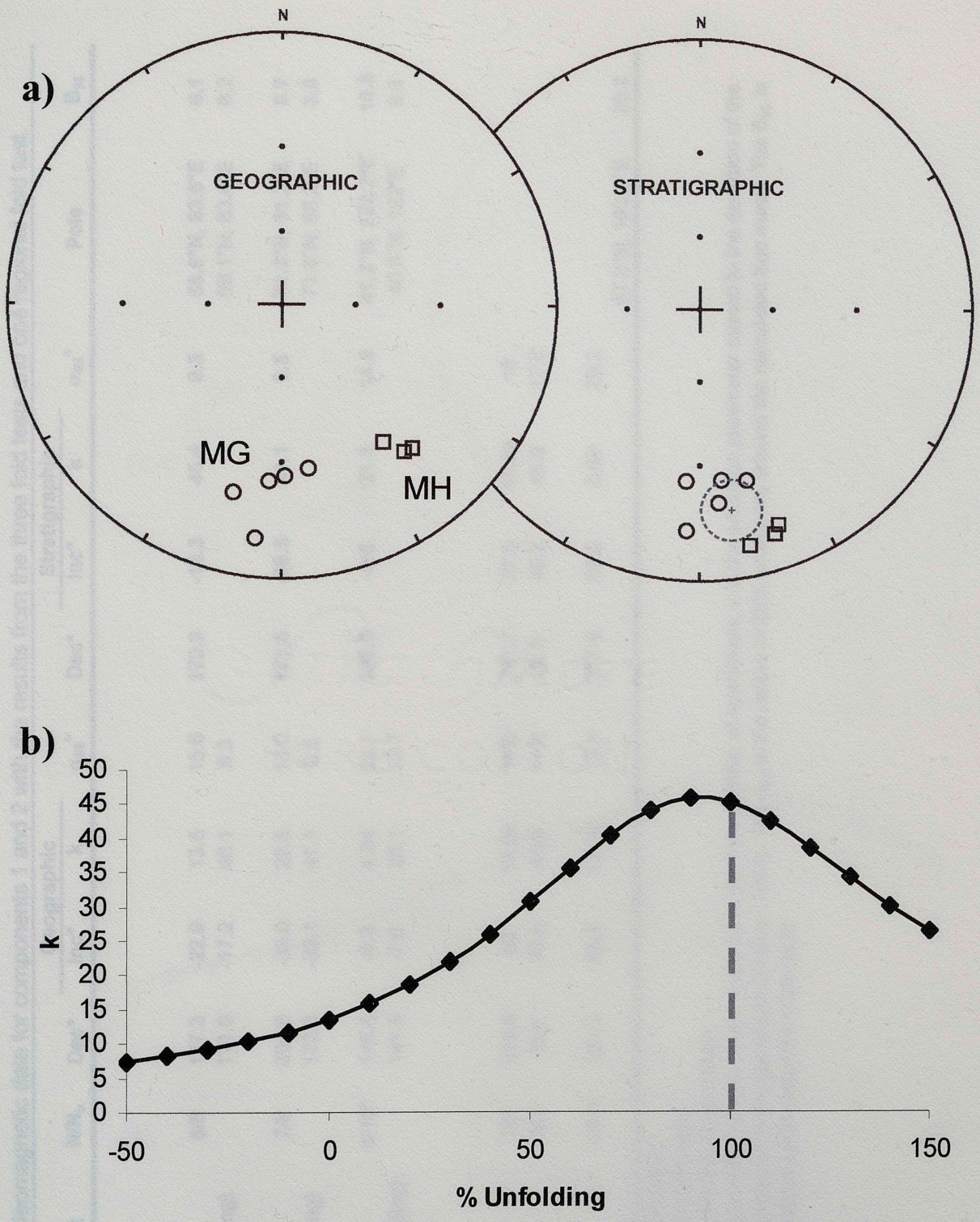

Figure 5: a) Equal area projection for component 1 site means in the Mountain Home Range in both geographic and stratigraphic positions (MG site, circles; MH site, squares). The open symbols represent negative inclinations. The dashed circle shows the α_{95} of the mean. b) Graph showing the percent unfolding versus grouping (k) for component 1 in the Mountain Home Range (Watson and Enkin, 1993). The best grouping is at 92% unfolding ±9%. The dashed line highlights the 100% unfolding position.

Table 2: Summary of paleomagnetic data for components 1 and 2 with the results from the three fold tests and one regional fold test.

Location/Component	N/N_o	Geographic Dec°	Geographic Inc°	Geographic k	Geographic α_{95}°	Stratigraphic Dec°	Stratigraphic Inc°	Stratigraphic k	Stratigraphic α_{95}°	Pole	B_{95}
Component 1											
Mountain Home Pass	8/8	167.3	-22.9	13.5	15.6	**170.9**	**-16.3**	**45.4**	**8.3**	**58.6°N, 83.6°E**	**6.1**
Best Grouping (92% unfolding)		171.0	-17.2	46.1	8.3					59.1°N, 83.6°E	6.2
Confusion Range	7/8	204.6	-30.0	22.5	13.0	**171.6**	**-38.9**	**41.1**	**9.5**	**71.3°N, 91.3°E**	**8.7**
Best Grouping (97% unfolding)		172.8	-39.1	41.1	9.5					71.8°N, 88.2°E	8.8
Stansbury Mountains	6/10*	146.6	-8.9	4.04	38.1	**142.0**	**-8.5**	**21.3**	**14.8**	**41.3°N, 122.2°E**	**10.6**
Best Grouping (121% unfolding)		141.8	-7.6	25.1	13.7					40.8°N, 122°E	9.8
Component 2											
Mountain Home Range	7/8	318.6	60	13.88	16.8	297.7	37.5	15.24	16		
Pavant Range	3/3	19.4	70.8	48.9	17.8	68.5	49.2	48.9	17.8		
Regional Fold Test	10/11	331.3	65.6	13.18	13.8	317.9	55.9	3.69	29.2		
Best Grouping (geographic)										67.3°N, 190.6°E	20.2

Bold values are for 100% unfolding.
Atipodes were not used in the fold tests.
*specimen directions used instead of site means
Note: N/N_o is the ratio of the number of specimens analyzed to the total number of specimens, k is the precision parameter related to the deviation of the true mean of the magnetic direction in the specimens (Fisher, 1953). The α_{95} is the radius of 95% probability around the calculated true mean. The B_{95} is the radius of the 95% confidence circle about the mean pole.

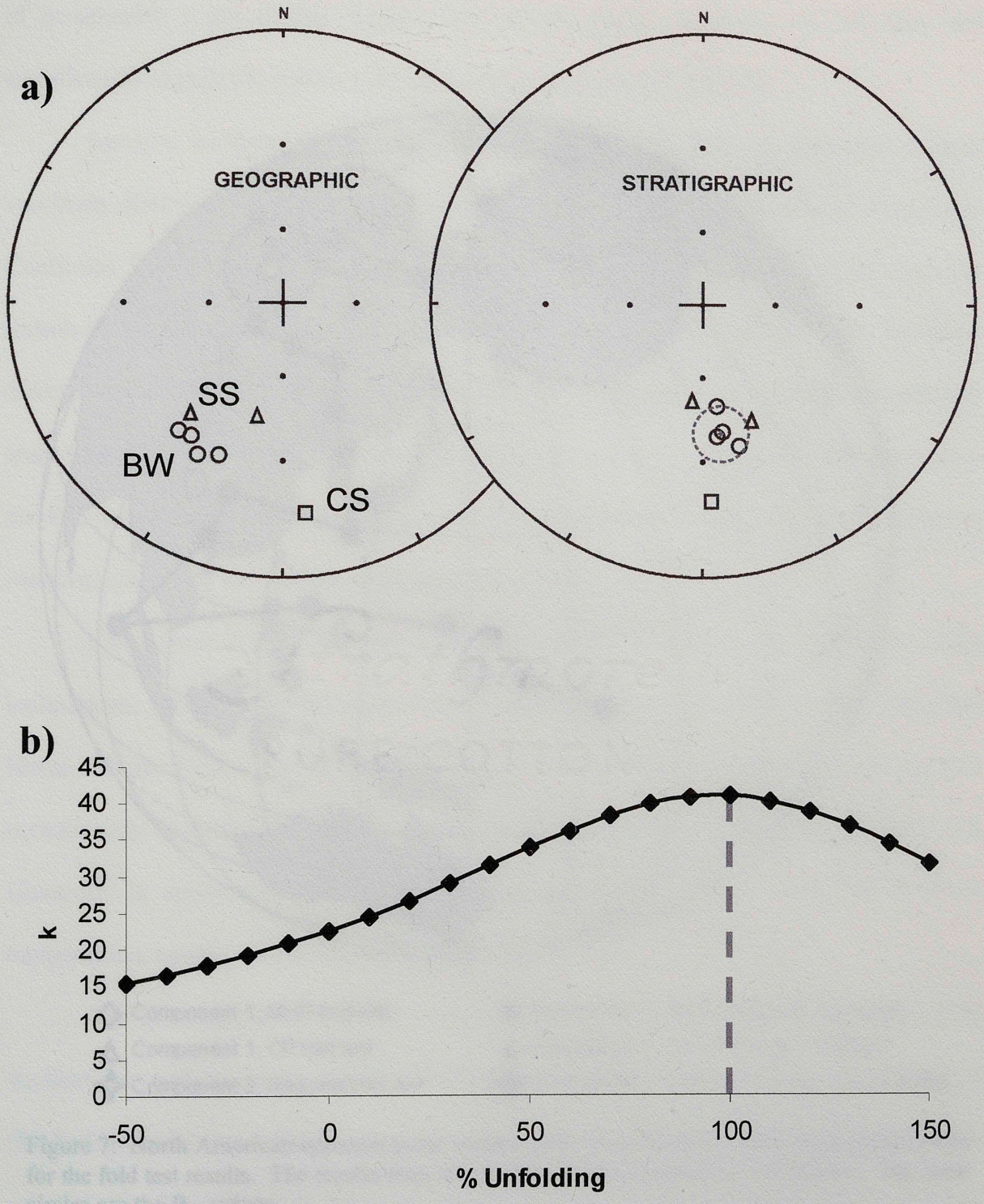

Figure 6: a) Equal area projection for component 1 site means in the Confusion Range in both geographic and stratigraphic positions. Site CS (squares) is on the east dipping limb, sites SS (triangles) and BW (circles) are on the west dipping limb. The open symbols represent negative inclinations. The dashed circle shows the α_{95} of the mean. b) Graph showing the percent unfolding versus grouping (k) for component 1 in the Confusion Range (Watson and Enkin, 1993). The best grouping is at 97% unfolding ±15%. The dashed line highlights the 100% unfolding position.

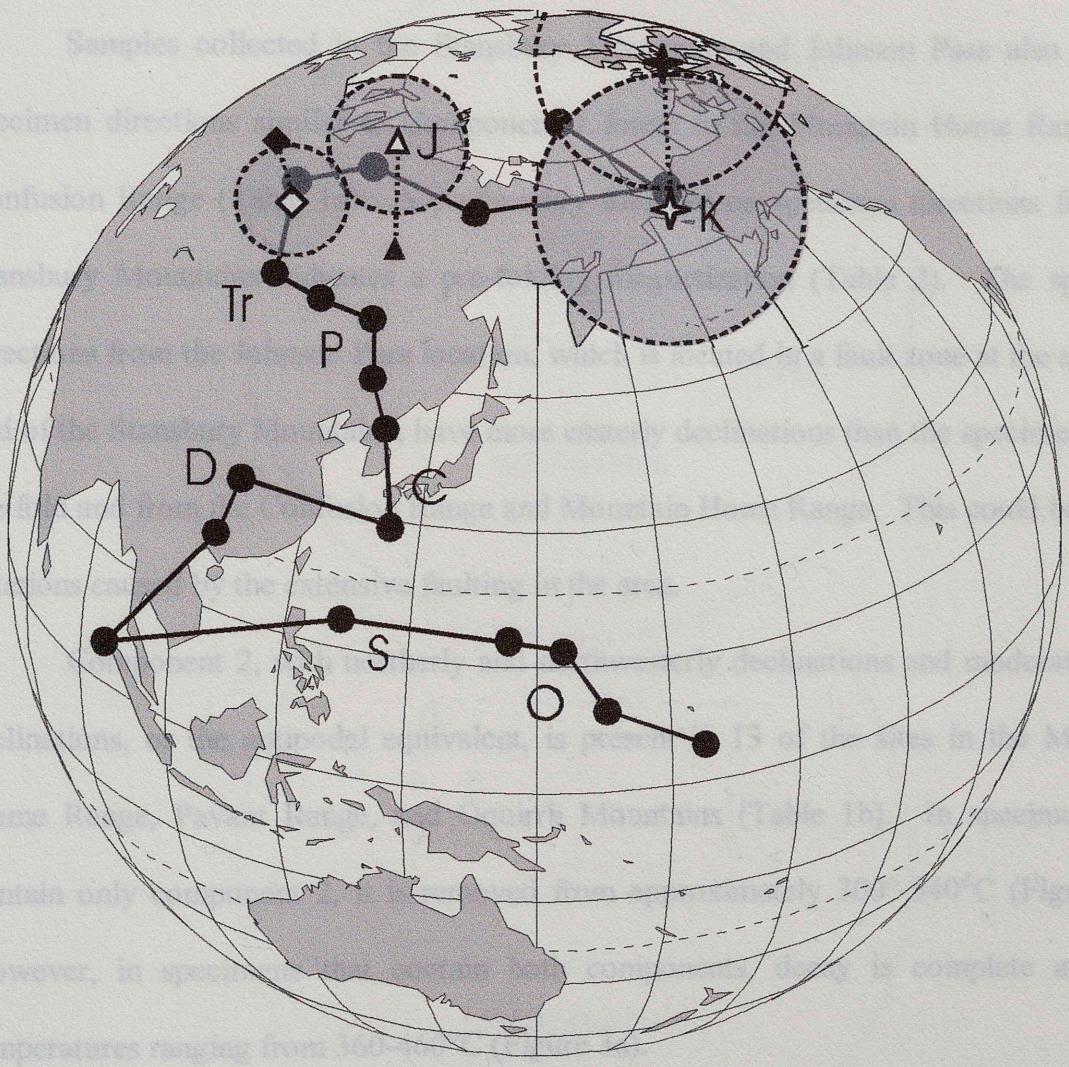

Figure 7: North American apparent polar wander path (Van der Voo, 1993) showing the poles for the fold test results. The results from the Tertiary tilt corrections are also shown. The error circles are the B_{95} values.

of component 1 are similar to the trend of the faults, removing the tilt does not significantly change the inferred age of the magnetizations (Figure 7).

Samples collected in the Stansbury Mountains and Johnson Pass also contain specimen directions similar to Component 1 found in the Mountain Home Range and Confusion Range (Table 1a). A preliminary fold test on specimen directions from the Stansbury Mountains indicates a pre-folding magnetization (Table 2). The specimen directions from the Johnson Pass location, which is located in a fault zone at the southern end of the Stansbury Mountains, have more easterly declinations than the specimens from the fold and from the Confusion Range and Mountain Home Range. This could be due to rotations caused by the extensive faulting in the area.

Component 2, with northerly and northwesterly declinations and moderate down inclinations, or the antipodal equivalent, is present in 13 of the sites in the Mountain Home Range, Pavant Range, and Oquirrh Mountains (Table 1b). In specimens that contain only component 2, it is removed from approximately 300°-540°C (Figure 3c). However, in specimens that contain both components, decay is complete at lower temperatures ranging from 360-460°C (Figure 3a).

The specimen directions from sites MG3, OPR1, and OPR2 have southeasterly declinations and moderate negative inclinations (Figures 3e and 8). A reversal test (McFadden and Lowes, 1981) was performed on the specimen directions from sites MG3 and the other MG sites and shows no distinction between the directions. A reversal test (McFadden and Lowes, 1981) was also performed on the site means from the OPR and MG sites with northwesterly declinations and again shows no distinction between the

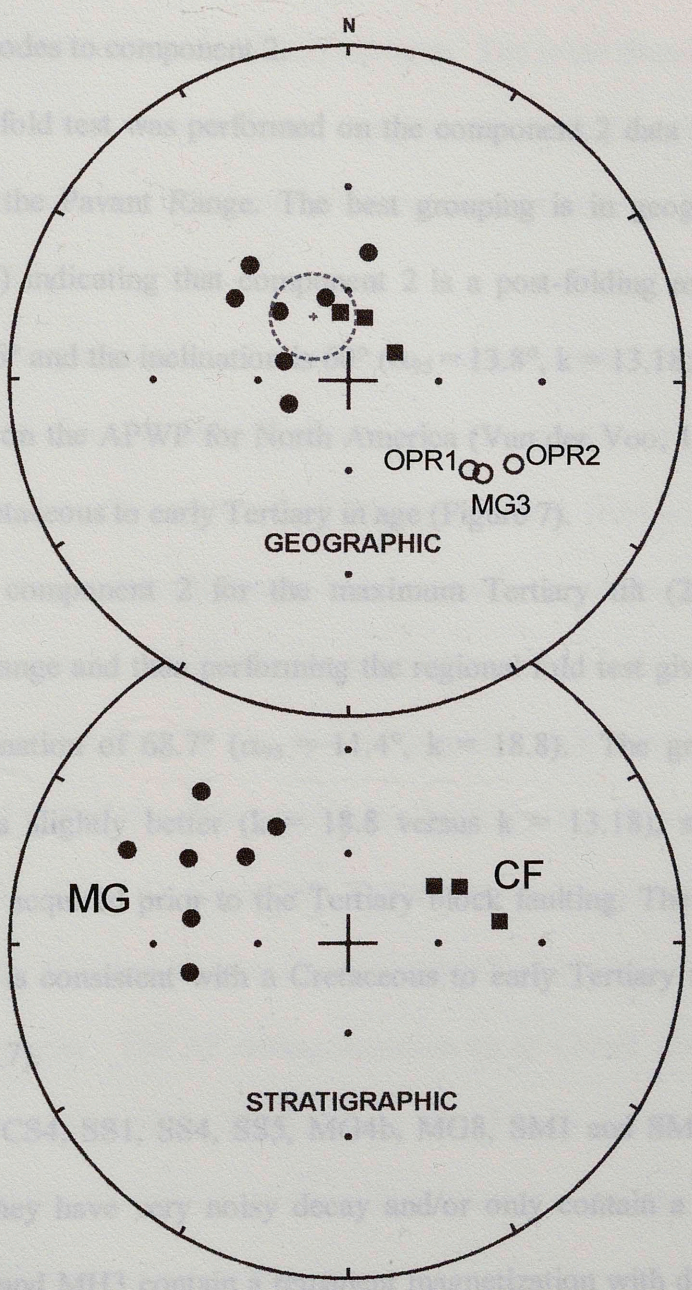

Figure 8: Equal area projections for component 2 site means. Regional fold test comparing geographic and stratigraphic site means from MG (circles) and CF (squares) sites. Site means of antipodes to component 2 (sites MG3, OPR1, OPR2) are shown but were not used in the regional fold test. The open symbols represent negative inclinations and closed symbols represent positive inclinations.

directions. Therefore, the specimen directions from sites MG3, OPR1, and OPR2 are interpreted as antipodes to component 2.

A regional fold test was performed on the component 2 data from the Mountain Home Range and the Pavant Range. The best grouping is in geographic coordinates (Figure 8; Table 2) indicating that component 2 is a post-folding magnetization. The declination is 318.6° and the inclination is 60° (α_{95} = 13.8°, k = 13.18; Table 2). Plotting the pole (Table 2) on the APWP for North America (Van der Voo, 1993) indicates that component 2 is Cretaceous to early Tertiary in age (Figure 7).

Correcting component 2 for the maximum Tertiary tilt (25 degrees) in the Mountain Home Range and then performing the regional fold test gives a declination of 12.7° and an inclination of 68.7° (α_{95} = 11.4°, k = 18.8). The grouping of the tilt-corrected values is slightly better (k = 18.8 versus k = 13.18), suggesting that the magnetization was acquired prior to the Tertiary block faulting. The new pole position (73.9°N, 276.6°E) is consistent with a Cretaceous to early Tertiary time of remanence acquisition (Figure 7).

Sites CS2, CS4, SS1, SS4, SS5, MG4b, MG8, SM1 and SM3 are not listed in Table 1 because they have very noisy decay and/or only contain a VRM component. Sites MH1, MH2, and MH3 contain a remanent magnetization with directions similar to component 1 in the other MH sites. However, these sites are also not shown in Table 1 because the specimen directions consistently have MAD angles greater than 15°.

Rock Magnetism

Low temperature analysis of 12 representative specimens shows a decrease in NRM intensity of 12.3 ± 6% after being subjected to liquid nitrogen. Thermal

demagnetization of these specimens does not show distinct directions when compared to specimens that were not subjected to liquid nitrogen. The small decrease in intensity and the fact that the directions do not change suggests that a significant amount of multi-domain grains with a modern VRM overprint are not present (e.g., Dunlop and Argyle, 1991, Halgedahl and Jarrard, 1995).

Thermal demagnetization of specimens suggests that the magnetization is contained in magnetite because decay is always complete at temperatures less that 580°C. This is also supported by the results of AF demagnetization, IRM acquisition, backfield measurements and triaxial thermal decay. In most specimens, AF demagnetization of the NRM up to 120mT shows a significant amount of decay (Figure 9a) which suggests that the magnetization is contained in low coercivity grains such as magnetite. The IRM acquisition up to 2500mT for these specimens typically shows saturation by 300mT (Figure 9b) which is typical for magnetite. Backfield measurements also show an initial decrease in intensity and then re-saturation by -300mT (Figure 9b). Saturation at low fields suggests magnetite. The AF demagnetization up to 120mT after IRM acquisition shows decay similar to that of the NRM (Figure 9a). Finally, the triaxial thermal decay of specimens shows that the low coercivity axis dominates and decays by 580°C (Figure 9c), indicating the presence of magnetite.

Although magnetite is the dominant magnetic phase in most specimens, the acquisition and thermal decay patterns for some specimens indicate the presence of other phases. In several specimens, for example, there is a decrease in intensity on the 500mT axis at approximately 320°C, suggesting that pyrrhotite is present (Figure 9c). Also, the magnetization in several specimens does not reach saturation by 2500mT (Figure 10a)

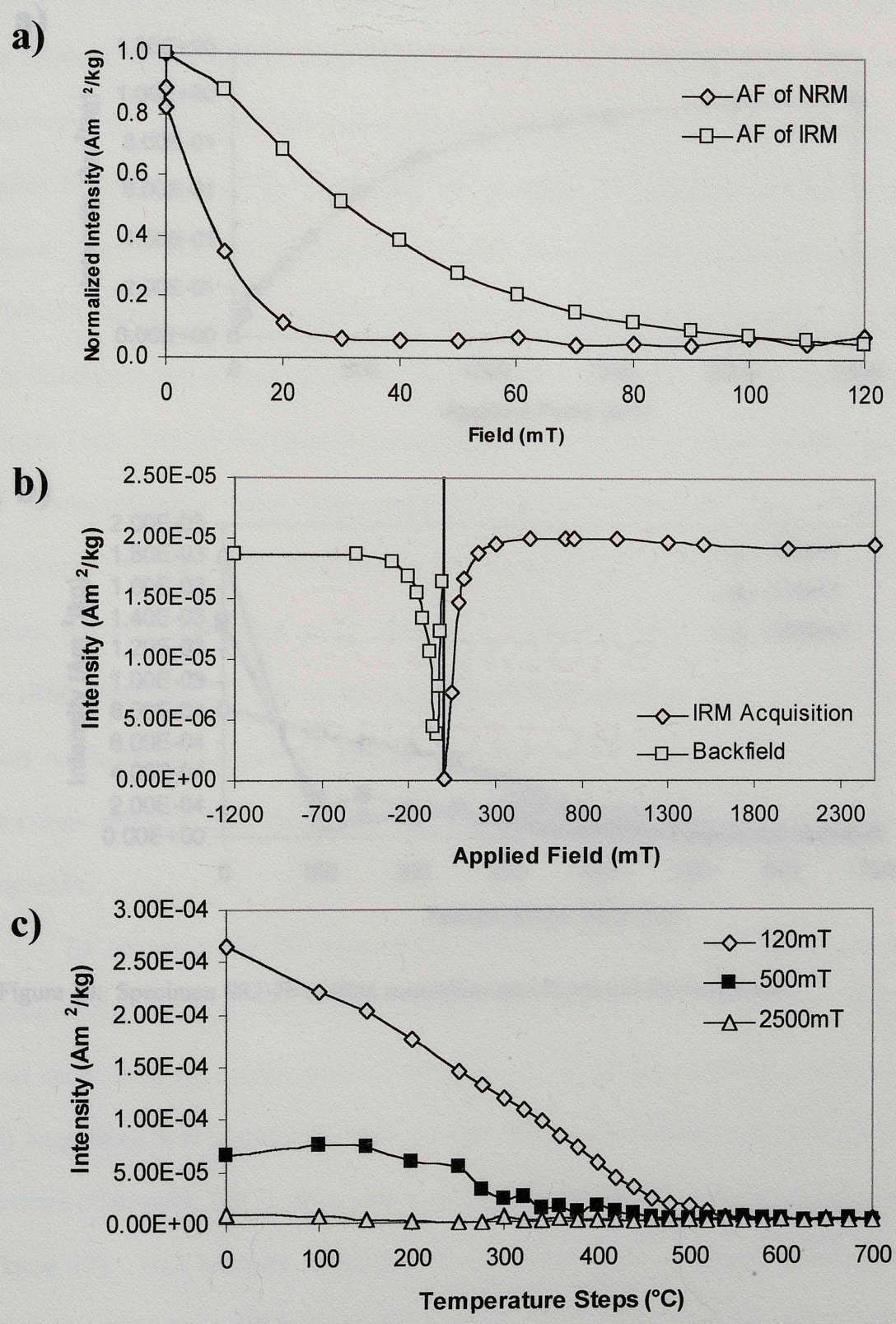

Figure 9: Specimen CS3-1b a) AF demagnetization of NRM and IRM, b) IRM acquisition and backfield, and c) triaxial thermal decay of IRM.

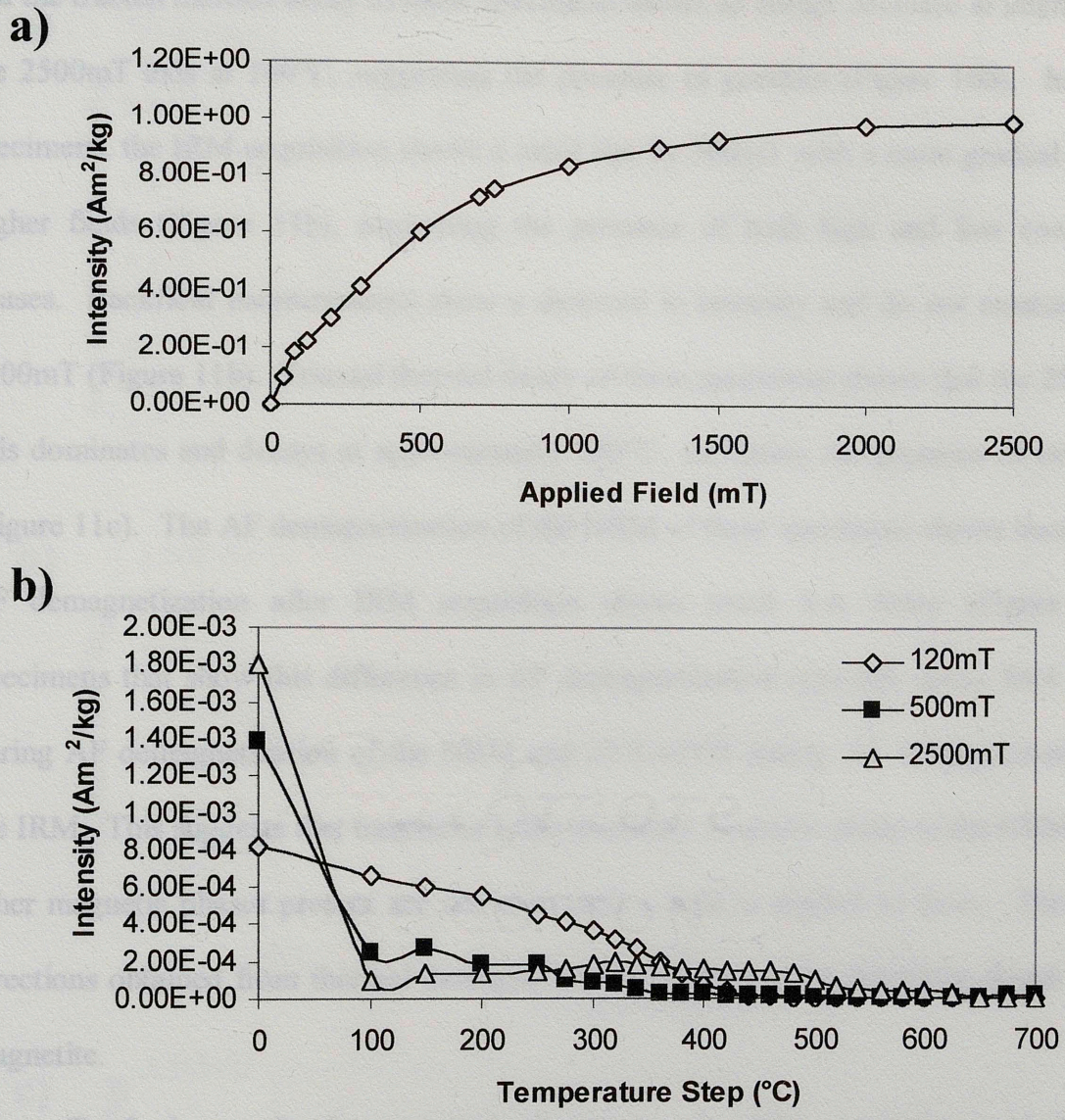

Figure 10: Specimen SS2-2b a) IRM acquisition and b) triaxial thermal decay.

and the triaxial thermal decay of these specimens shows an abrupt decrease in intensity of the 2500mT axis at 100°C, suggesting the presence of goethite (Figure 10b). In other specimens, the IRM acquisition shows a rapid rise by 300mT with a more gradual rise at higher fields (Figure 11b), suggesting the presence of both high and low coercivity phases. Backfield measurements show a decrease in intensity and do not resaturate by 1200mT (Figure 11b). Triaxial thermal decay of these specimens shows that the 2500mT axis dominates and decays at approximately 680°C, indicating the presence of hematite (Figure 11c). The AF demagnetization of the NRM of these specimens shows decay, but AF demagnetization after IRM acquisition shows much less decay (Figure 11a). Specimens that show this difference in AF demagnetization typically decay 84.4 ±14% during AF demagnetization of the NRM and 27.7 ±11% during AF demagnetization of the IRM. This suggests that magnetite is the dominant magnetic phase in the NRM. The other magnetic phases present are not seen until a field is applied to them. Therefore, directions obtained from thermal demagnetization represents the directions found in the magnetite.

To further study the magnetic mineralogy, the IRM acquisition and the AF demagnetization of the IRM were compared in crossover plots (Cisowski, 1981). For most specimens, the curves intersect between 40 and 50% normalized moment (Figure 12) suggesting non-interacting single domain (SD) and/or pseudosingle domain (PSD) particles (Cisowski, 1981). In addition, crossover typically occurs between 40 and 60mT (Figure 12). This behavior suggests that magnetite is the dominant remanence carrier (Symons and Cioppa, 2000). The IRM decay curves of these specimens have inflected shapes which, according to Dunlop (1983), is representative of SD or PSD behavior

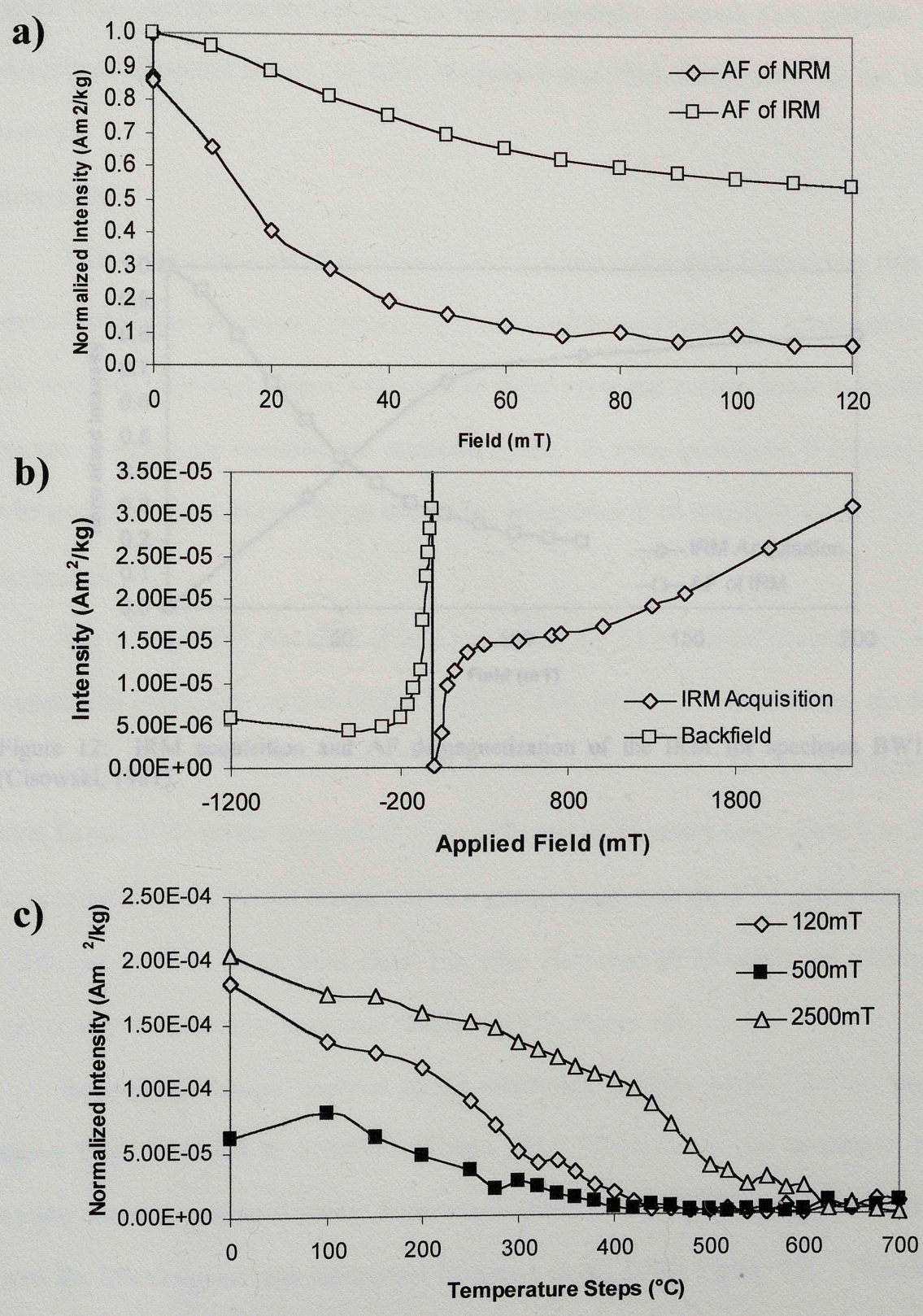

Figure 11: Specimen MH5-6a a) AF demagnetization of NRM and IRM , b) IRM acquisition and backfield, and c) triaxial thermal decay of IRM.

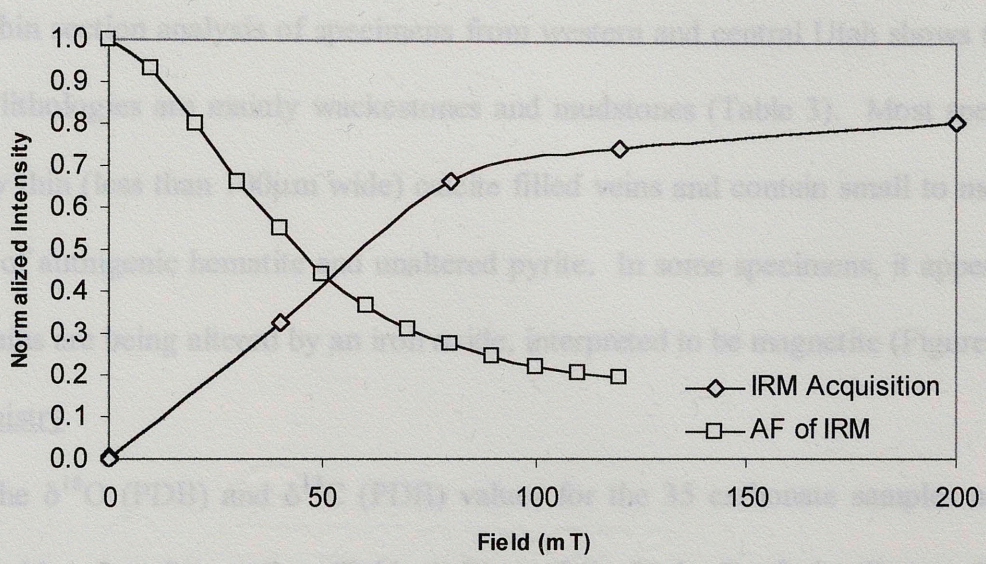

Figure 12: IRM acquisition and AF demagnetization of the IRM for specimen BW1-7 (Cisowski, 1981).

(Figure 12). For specimens that contain higher coercivity minerals (i.e., goethite and hematite) as discussed above, the IRM acquisition and IRM decay curve do not show crossover.

Petrography

Thin section analysis of specimens from western and central Utah shows that the sampled lithologies are mainly wackestones and mudstones (Table 3). Most specimens have very thin (less than 100μm wide) calcite filled veins and contain small to moderate amounts of authigenic hematite and unaltered pyrite. In some specimens, it appears that pyrite grains are being altered by an iron oxide, interpreted to be magnetite (Figure 13).

Geochemistry

The $\delta^{18}O$ (PDB) and $\delta^{13}C$ (PDB) values for the 35 carbonate samples are well grouped with only a few outliers (Table 4; Figure 14). In the Confusion Range, the $\delta^{18}O$ values range from -5 to -2‰ and $\delta^{13}C$ values range from -1.5 to 3‰. In the Mountain Home Range $\delta^{18}O$ values range from -6 to -4‰ and $\delta^{13}C$ values range from 0 to 2‰. The samples from the Pavant Range exhibit a greater range with the $\delta^{18}O$ values from -10 to -2‰ and the $\delta^{13}C$ values from about 1 to 4‰. However, all 35 values fall within the range common for marine limestones (Hudson, 1977; Figure 14).

Radiogenic isotope analysis of 12 carbonate samples yield $^{87}Sr/^{86}Sr$ values ranging from 0.707649 to 0.708112 (Figure 15). These values are consistent with seawater curves constructed mainly from samples from the southern interior of the United States for Mississippian age limestones (Denison et al., 1994; Figure 15). Therefore, these samples closely represent the $^{87}Sr/^{86}Sr$ ratios of seawater at the time the Deseret Limestone and Chainman Shale were deposited. This similarity suggests that the samples

have not been altered by externally derived fluids which are commonly enriched in ^{87}Sr (e.g., Stueber et al., 1984; Chaudhuri et al., 1987; Clauer et al., 1989).

Table 3: Classification and diagenetic features from thin section analysis of petrographic samples

Specimen	Classification	Diagenetic Features
CF1	wackestone	calcite filled veins (20-75μm wide)
CF2	wackestone	calcite filled veins (50-600μm wide)
CS1-2	fossiliferous wackestone	thin calcite filled vein, moderate amount authigenic hematite
CS2-1	wackestone	moderate amount authigenic hematite, calcite filled vein
CS3-6	wackestone	thin calcite filled vein, small amount pyrite
CS4-3	fossiliferous grainstone	thin calcite filled veins, moderate amount authigenic hematite
BW1-3	fossiliferous wackestone	moderate amount authigenic hematite, hematite replacing pyrite
BW2	fossiliferous wackestone	calcite filled veins (~80μm wide), authigenic hematite, hematite filled veins
BW3-2	fossiliferous wackestone	calcite filled vein (100μm wide), unaltered pyrite (~100μm grains)
BW4-1	packstone	calcite filled vein (80μm wide), unaltered pyrite, authigenic hematite, hematite replacing pyrite
SS1-2	wackestone	pyrite grains (~5μm)
SS2-3	wackestone	moderate amount authigenic hematite, hematite replacing pyrite
SS2-3	wackestone	moderate amount authigenic hematite, hematite replacing pyrite
SS3-4	wackestone	calcite filled veins (~10μm wide), pyrite and authigenic hematite
MH4-1	mudstone	calcite filled vein (80μm wide), veins (~600mm wide) with large amount of hematite along edges, possibly hydrocarbons
MH5-3	mudstone	thick (~2000mm wide) calcite filled vein, several small (~50mm) calcite filled veins, small amount authigenic hematite and pyrite
MH6-3	mudstone	very small amount authigenic hematite, small amount pyrite, hematite replacing pyrite
MG1-1	fossiliferous wackestone	moderate amount authigenic hematite
MG2-4	fossiliferous wackestone	moderate amount authigenic hematite, hematite filled vein
MG3-3	wackestone	small amout authigenic hematite
MG4a-2	fossiliferous wackestone	moderate amount authigenic hematite, hematite filled vein
MG4b-3	wackestone	moderate amount authigenic hematite
MG5-1	fossiliferous wackestone	small amout authigenic hematite
MG6-10	fossiliferous wackestone	moderate amount authigenic hematite
MG7-2	wackestone	moderate amount authigenic hematite
MG9	mudstone	calcite filled veins (70-1200μm wide), small amount authigenic hematite, possibly very fine grained pyrite and magnetite
JNP2-1	mudstone	very thin calcite filled veins

Figure 13: Thin section showing magnetite replacing pyrite in reflected light.

Table 4: Stable isotope values.

Specimen	$\delta^{13}C$ (PDB)	$\delta^{18}O$ (PDB)
BW1-2	1.16	-2.38
BW2	1.16	-2.58
BW3-3	1.95	-3.51
BW4-2	1.56	-3.64
CS1-4	-0.55	-3.5
CS2-3	-0.73	-2.61
CS3-5	-0.76	-3.38
CS4-5	-1.16	-3.18
SS1	1.95	-3.6
SS2-5	2.67	-3.59
SS3-4	2.1	-3.34
SS4-3	1.6	-5.09
SS5-1	1.49	-5
MG1-7	1.07	-5.09
MG2-2	0.75	-5.41
MG3-5	1.3	-4.61
MG4a-4	1.32	-4.52
MG5-2	1.25	-3.59
MG6-1	0.9	-4.97
MG7	1.86	-4.83
MG8-1	0.23	-5.84
MG9-4	1.8	-4.18
MG10-2	0.19	-6.2
MH1	0.53	-5.1
MH2-1	0.5	-4.84
MH3-4	0.54	-5.7
MH4-5	0.43	-4.91
MH5-3	0.2	-5.5
MH6-1	0.32	-5.43
CF1	2.52	-4.87
CF2-3	1.17	-10.16
CF1-2	2.22	-8.68
CF1-3	2.24	-9.27
CF3-4	3.44	-2.08
CF3-6	3.33	-2.84

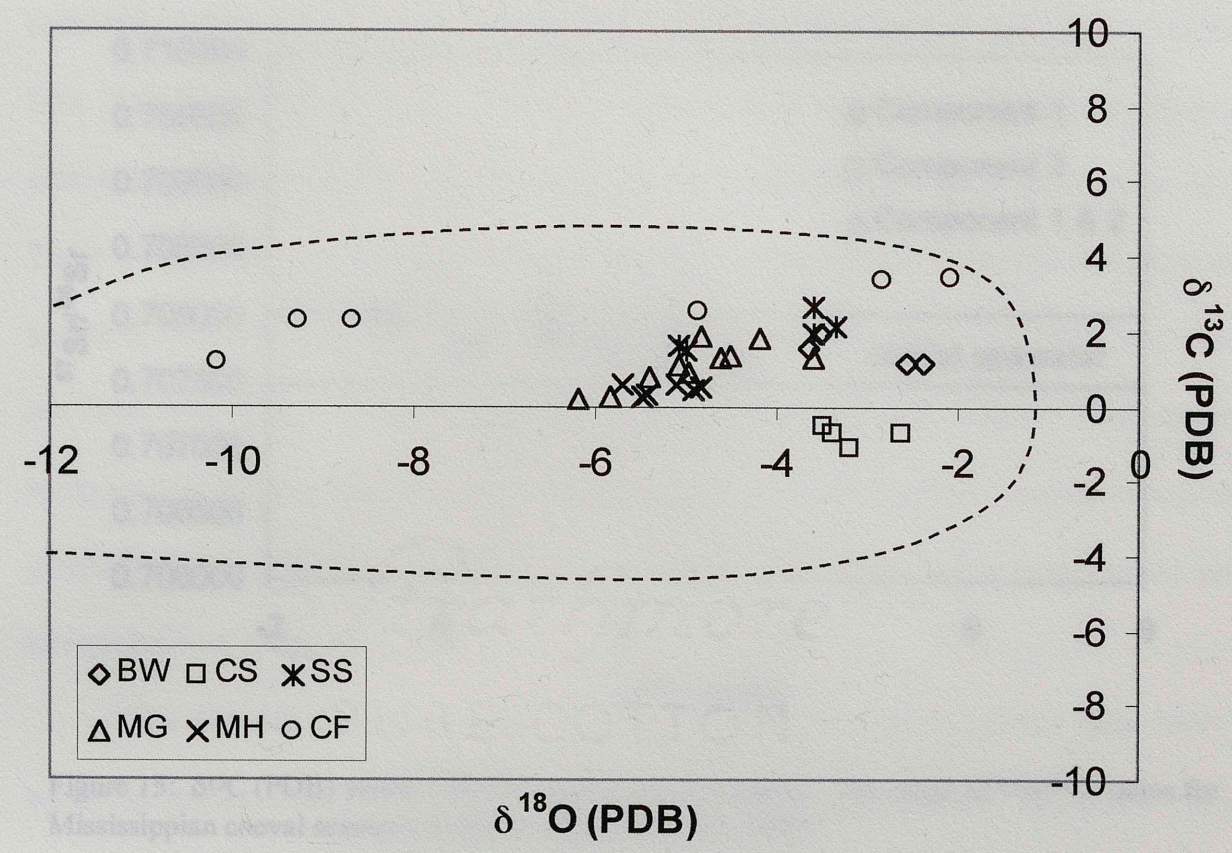

Figure 14: Plot of stable isotope data for the 35 carbonate samples. The different symbols correspond to the locations from which the samples were collected. The dashed line represents the range of common marine limestones after Hudson (1977).

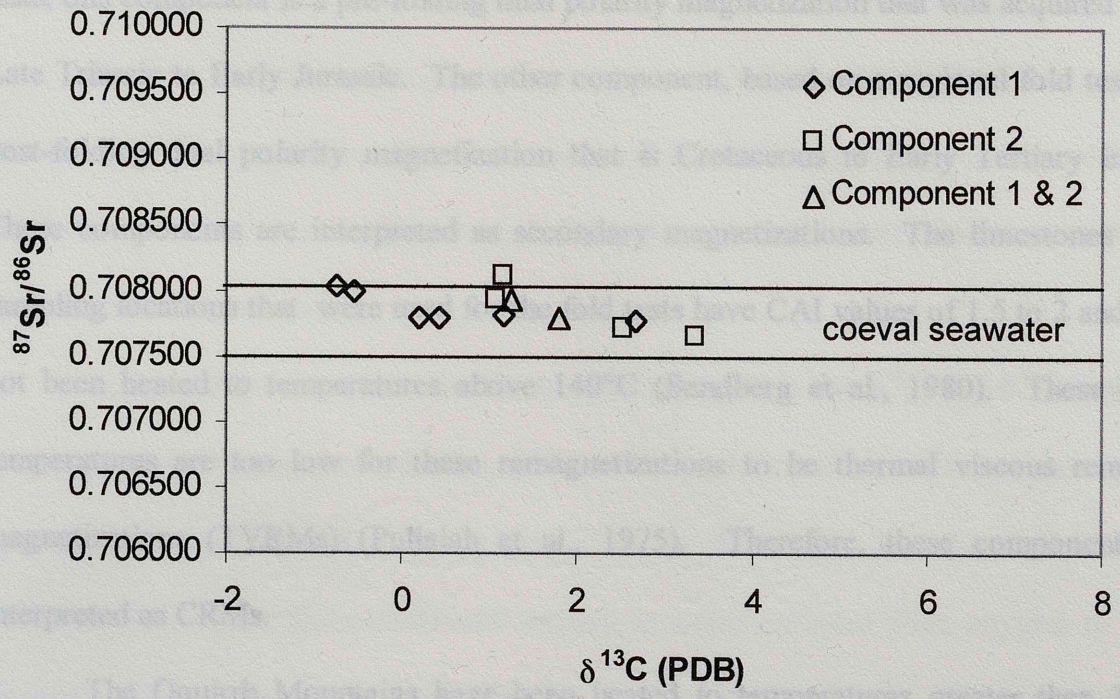

Figure 15: $\delta^{13}C$ (PDB) versus $^{87}Sr/^{86}Sr$ values for 12 samples. The range of $^{87}Sr/^{86}Sr$ ratios for Mississippian coeval seawater is shown (Denison et al., 1994).

DISCUSSION

The samples of the Mississippian Deseret Limestone and Chainman Shale collected in western and central Utah contain two ancient components. Based on fold tests, one component is a pre-folding dual polarity magnetization that was acquired in the Late Triassic to Early Jurassic. The other component, based on a regional fold test, is a post-folding dual polarity magnetization that is Cretaceous to Early Tertiary in age. These components are interpreted as secondary magnetizations. The limestones at all sampling locations that were used for the fold tests have CAI values of 1.5 to 2 and have not been heated to temperatures above 140°C (Sandberg et al., 1980). These burial temperatures are too low for these remagnetizations to be thermal viscous remanent magnetizations (TVRMs) (Pullaiah et al., 1975). Therefore, these components are interpreted as CRMs.

The Oquirrh Mountains have been heated to temperatures greater than 300°C which is higher than the temperatures at the locations used in the fold tests. The specimens from the Oquirrh Mountains typically decay above 500°C and some decay at 580°C. This suggests that the magnetization in these sites is a CRM (Pullaiah et al., 1975). However, this interpretation is ambiguous because the maximum temperature is not known. If the rocks were heated higher than 450°C, the magnetization could be a TVRM. In addition, Melker and Geissman (1997) have found a primary magnetization in the Tertiary intrusive and extrusive igneous rocks in the Oquirrh Mountains.

Both CRMs contain normal and reversed directions. The inferred age for the pre-folding component 1 CRM is consistent with the polarity changes in the Late Triassic and Early Jurassic (Butler, 1992). The normal and reversed directions in the post-folding

CRM are also consistent with the polarity changes in the Late Cretaceous and early Tertiary (Butler, 1992). The presence of dual polarity magnetizations indicates that the CRMs were acquired over long enough periods to experience both normal and reversed polarities.

The results from the rock magnetism analysis indicate that both CRMs reside in SD and/or PSD magnetite. Small amounts of pyrrhotite, goethite, and hematite are present is some specimens. However, it does not appear that these phases contribute to the remanent magnetization.

The geochemical results for the samples plot within the $\delta^{18}O$ and $\delta^{13}C$ range for common marine limestones (Hudson, 1977). The variation in the $\delta^{18}O$ values could be caused by re-equilibration with meteoric water or differences in original depositional environment. Also, since carbonate carbon is more resistant than oxygen to post-depositional exchange processes effecting limestones (Keith and Weber, 1964), the variation in the $\delta^{13}C$ values is likely due to a variable depositional environment rather than chemically altering fluids. Specimens also contain very thin calcite veins. However, these veins are not necessarily the result of externally derived fluids and can have $\delta^{13}C$ values similar to those of the host rock (Gao et al., 1992). Previous studies suggest that $\delta^{13}C$ values are depleted in rocks that have been altered by externally derived fluids (Gao et al., 1992). This depletion is not observed and the range of isotopic values suggests that the rocks with the CRMs have not been chemically altered by externally derived fluids.

A previous geochemical study on the Delle shows that the $\delta^{18}O$ values of the Delle event rocks are 3-5‰ lighter than the underlying and overlying open-marine

limestones (Jewell et al., 2000). This $\delta^{18}O$ data (along with Sr and Mn data) led them to interpret the Delle rocks as being deposited in a restricted environment. In the present study, the data from the Pavant Range shows evidence for the Delle isotopic signature as described by Jewell et al. (2000). Three of the specimens have $\delta^{18}O$ values that are more depleted than the other specimens in the study. The $\delta^{18}O$ depletion in this study is interpreted to be the result of isotopic variations due to depositional environment rather than chemically altering fluids, which is similar to the interpretations by Jewell et al. (2000).

Radiogenic isotope analysis shows that $^{87}Sr/^{86}Sr$ values for the samples are similar to $^{87}Sr/^{86}Sr$ values from seawater curves for Mississippian age carbonates. These similarities suggest that the rocks have not been altered by externally derived fluids.

Petrographic analyses identified pyrite grains being altered to an iron oxide interpreted to be magnetite. Previous studies have also noted pyrite grains altered to an iron oxide in association with the presence of CRMs (e.g., Fruit et al., 1995; Weil and Van der Voo, 2002). Therefore, it is inferred that the magnetite seen in thin section may carry one or both of the CRMs.

The relationship between the magnetization and timing of the oil window can be seen (Figure 16) by comparing the age of the CRMs to the time versus vitrinite reflectance curve from Huntoon et al. (1999). Component 1 plots at the beginning of the oil window. The age of the CRM is prior to the onset of the Sevier orogeny and the geochemical and petrographic analysis provides no evidence for fluid alteration, suggesting that this CRM could be related to an early burial diagenetic process. Component 2 plots toward the end of the oil window (Figure 16). This CRM is post-

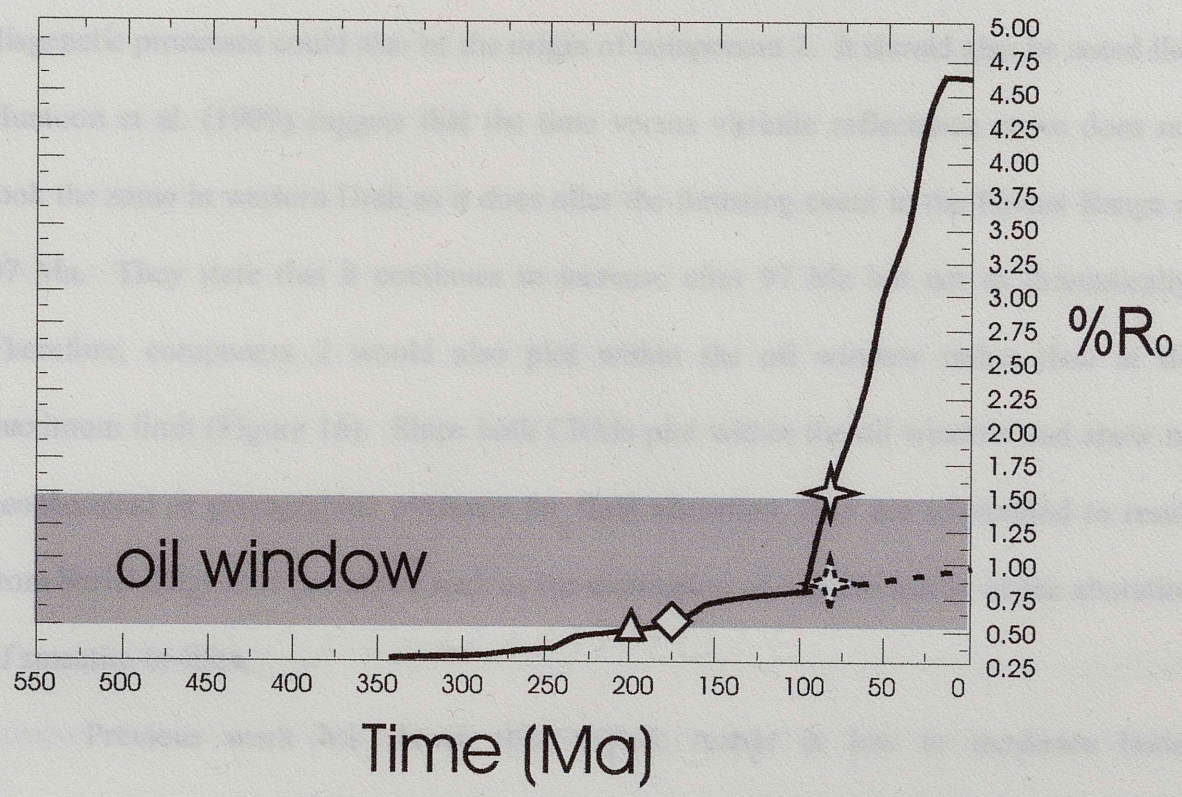

Figure 16: Time versus vitrinite reflectance curve for the Mississippian Deseret Limestone (modified from Huntoon et al., 1999) with the oil window. The triangle (CR) and diamond (MHR) represent the Late Triassic to Early Jurassic component 1 and the star represents the Cretaceous to early Tertiary Component 2. The dashed line represents the estimated curve for the Chainman Shale in western Utah and the dashed star represents component 2 on the estimated curve.

folding and the timing (Cretaceous to early Tertiary) coincides with the Sevier and Laramide orogenies. However, geochemical and petrographic analyses indicate that externally derived fluids have not passed though the rock. This suggests that burial diagenetic processes could also be the origin of component 2. It should also be noted that Huntoon et al. (1999) suggest that the time versus vitrinite reflectance curve does not look the same in western Utah as it does after the thrusting event in the Pavant Range at 97 Ma. They state that it continues to increase after 97 Ma but not as dramatically. Therefore, component 2 would also plot within the oil window rather than at the maximum limit (Figure 16). Since both CRMs plot within the oil window and show no geochemical or petrographic evidence for fluid alteration, they are interpreted to result from burial diagenetic processes such as the maturation of organic matter or the alteration of smectite-to-illite.

Previous work has shown that organic matter at low to moderate burial temperatures causes magnetite authigenesis and an associated CRM. For example, Plaster-Kirk et al. (1995) found a CRM residing in magnetite in organic-rich lacustrine deposits of the Middle Old Red Sandstone in Scotland. The Carboniferous age of the CRM correlates with the suggested time of organic matter maturation (Plaster-Kirk et al., 1995). Banerjee et al. (1997) found a pre-folding to syn-folding CRM in authigenic magnetite from carbonates of the Pennsylvanian Belden Formation in Colorado. The age of the CRM varies from late Paleozoic to Cretaceous and coincides with the modeled time of organic matter maturation in different parts of the basin. This CRM was interpreted as forming from magnetite authigenesis caused by diagenetic reactions that were triggered by low to moderate burial temperatures (Banerjee et al., 1997). Cioppa et

al. (2002) related a CRM in the "Nordegg Member" of the Fernie Formation in Canada to organic matter maturation of the organic-rich shales. In addition, Brothers et al., (1996) conducted simulation experiments to demonstrate that authigenic magnetite can form from pyrite in the presence of organically complex ferric iron that can act as an oxidizing agent at temperatures of about 90°C.

Clay alteration, specifically the smectite-to-illite transition, occurs in the same temperature range as hydrocarbon generation (Pevear, 1999) and CRMs have been associated with the smectite-to-illite transition in which illitization releases iron to form authigenic magnetite (Katz et al., 2000). Katz et al. (2000) found a CRM carried by magnetite in the Jurassic and Cretaceous carbonates of the Vocontian trough in southeast France. The CRM was found in locations where smectite had been altered to other clay minerals. However, the CRM was absent or weak in locations where a significant amount of smectite was still present. There was no geochemical evidence for orogenic fluids and, therefore, it was interpreted that the origin of the widespread CRM was burial diagenesis of smectite (Katz, et al., 2000). Gill et al. (2002) used a similar presence-absence test in the Ovethrust Belt of Montana to show the connection between the timing of a CRM and the smectite-to-illite conversion. Laboratory simulation experiments are also consistent with a connection between clay diagenesis and magnetite authigenesis (Hirt et al., 1993; Cogoini et al., 2002).

The origin of pervasive CRMs has been controversial and is unresolved. In addition to burial diagenetic processes, fluids activated as a result of orogenic activity (e.g., Oliver, 1992) are commonly hypothesized as an agent of remagnetization. Evidence for the orogenic fluid hypothesis includes a spatial connection between

orogenic belts and the rocks that contain the CRMs, and a temporal connection between the timing of remagnetization and tectonic events. In some cases the orogenic fluid model is a reasonable interpretation, particularly for those localized CRMs near or in conduits for flow (Elmore et al., 1999; Elmore, 2001). However, many units such as the Deseret Limestone contain pervasive CRMs but do not contain geochemical evidence for alteration by externally derived fluids (e.g., Elmore et al., 1993; Elmore, 2001). These CRMs, therefore, are probably related to another widespread diagenetic mechanism such as a burial diagenetic process.

The agreement of the timing of remagnetization and maturation of organic matter in the Deseret Limestone and Chainman Shale suggest that the CRMs are probably associated with the maturation of organic matter. However, clay alteration cannot be excluded as a possible alternative mechanism because both processes occur under the same conditions.

The component 1 CRM in western Utah is apparently older than the component 2 CRM in central/western Utah. This suggests a trend with the CRMs getting younger to the east. This interpretation should be viewed with caution, however, because it is based on the regional fold test for the component 2 CRM and the timing of folding in western and central Utah were different (Heller et al., 1986). Thrusting in Utah moved from west to east during the Sevier orogeny. Assuming that the regional trend is valid, it is interesting to compare this apparent trend with that noted in other studies which have identified remagnetization trends perpendicular to thrust fronts (e.g., Stamatakos et al., 1996; Enkin et al., 2000). This apparent trend in Utah is similar to results from the southern Canadian Cordillera in which older remagnetizations were found in the

hinterland and younger magnetizations were found in the foreland (Enkin et al., 2000). The apparent trend, however, is opposite to the trend observed by Stamatakos et al. (1996) in the central Appalachians where post-folding magnetizations were noted in the hinterland and pre-folding in the foreland. A more thorough discussion of the significance of the apparent trend observed in this study will require confirmation of its validity.

The Triassic to Jurassic age of component 1 is unusual compared to previous studies in North America (McCabe and Elmore, 1989). In addition, the component 1 CRM is pre-folding which is relatively unusual considering that most CRMs that reside in magnetite in folded rocks are syn-folding. Several studies have suggested that these CRMs are truly syn-folding and are related to fluids activated during orogenesis (e.g., McCabe et al., 1983; Elmore et al., 2001). Other studies, however, have proposed that the syn-folding character is only apparent and that the magnetization has been altered, perhaps by strain during folding (e.g., Lewchuk et al., 2002). Assuming that strain is a factor in causing some syn-folding magnetizations, it is interesting to speculate why the Deseret Limestone does not exhibit a syn-folding character. One reason could be that the rocks sampled were micritic limestones interbedded with shales. In this situation, the shales would reduce the amount of strain on the limestones, therefore preventing a syn-folding fold test result.

CONCLUSIONS

There are two ancient remanent magnetizations in the Mississippian Deseret Limestone and Chainman Shale in western and central Utah. Both components are secondary CRMs that reside in magnetite. Fold test results suggest that one CRM is a dual polarity pre-folding magnetization that is Late Triassic to Early Jurassic in age and the other is a dual polarity post-folding magnetization that is Cretaceous to early Tertiary in age. Comparing the ages of the CRMs to burial data, it appears that the pre-folding and post-folding CRMs could be the result of burial diagenetic processes such as maturation of organic mater and/or clay alteration. Geochemical and petrographic analyses do not indicate alteration by externally derived fluids.

The results of this study support the hypothesis that pervasive CRMs are associated with widespread burial diagenetic mechanisms such as maturation of organic matter and clay alteration. In addition, the results suggest that paleomagnetism can be used to determine the timing of these burial diagenetic processes which, when combined with conventional maturation data (i.e., conodont alteration, vitrinite reflectance, and burial curves), would benefit exploration efforts and help determine the viability of a potential source rock.

REFERENCES

Baer, J.L., Davis, R.L., and George, S.E., 1982, Structure and stratigraphy of the Pavant Range, central Utah, *Overthrust Belt of Utah: Symposium and Field Conference*, Utah Geological Association, Publication 10, pp. 31-48.

Banerjee, S., Engel, M., and Elmore, R.D., 1997, Chemical remagnetization and burial diagenesis: Testing the hypothesis in the Pennsylvanian Belden Formation, Colorado, *Journal of Geophysical Research*, v. 102, pp. 24825-24842.

Beratan, K.K., ed., 1996, Reconstructing the history of Basin and Range extension using sedimentology and stratigraphy, *Geological Society of America Special Paper 303*.

Bird, P., 1998, Kinematic history of the Laramide orogeny in latitudes 35°-49°N, western United States, *Tectonics*, v. 17, no. 5, pp. 780-801.

Brothers, L.A., Engel, M.H., and Elmore, R.D., 1996, The late diagenetic conversion of pyrite to magnetite by organically complexed ferric iron, *Chemical Geology*, v. 130, pp. 1-14.

Butler, R.F., 1992, *Paleomagnetism: magnetic domains to geologic terranes*, Blackwell Science Inc., Boston, MA, 319 pp.

Chaudhuri, S., Broedel, V., and Clauer, N., 1987, Strontium isotopic evolution of oil-field waters from carbonate reservoir rocks in Bindley field, Central Kansas, USA, *Geochimica et Cosmochimica Acta*, v. 51, pp. 45-53.

Cioppa, M.T., Symons, D.T.A., and Flore, M., 2002, Initial analysis of the Jurassic "Nordegg Member," Fernie Formation: using paleomagnetism to date source rock thermal maturation, *Physics and Chemistry of the Earth*, v. 27, pp. 1161-1168.

Cisowski, S., 1981, Interacting vs. non-interacting single domain behavior in natural and synthetic samples, *Physics of the Earth and Planetary Interiors*, v. 26, pp. 56-62.

Clauer, N., Chaudhuri, S., and Subramanium, R., 1989, Strontium isotopes as indicators of diagenetic recrystallization scales within carbonate rocks, *Chemical Geology*, v. 80, pp. 27-34.

Cogoini, M., Elmore, R.D., and Engel, M., 2002, Thermal treatment of clays resulting in magnetic mineral formation in a smectite - An analogy to low burial conditions, *American Geophysical Union*, Fall Meeting, Abstract.

Denison, R.E., Koepnick, R.B., Burke, W.H., Hetherington, E.A., and Fletcher, A., 1994, Construction of the Mississippian, Pennsylvanian and Permian seawater $^{87}Sr/^{86}Sr$ curve, *Chemical Geology*, v. 112, pp. 145-167.

Dunham, R.J., 1962, Classification of carbonate rocks according to depositional texture, *AAPG Memoir*, no. 1, pp. 108-121.

Dunlop, D.J., 1983, Determination of domain structure in igneous rocks by alternating field methods, *Earth and Planetary Science Letters*, v. 63, pp. 353-357.

Dunlop, D.J., and Argyle, K.S., 1991, Separating multidomain and single-domain-like remanences in pseudo-single-domain magnetites (215-540nm) by low-temperature demagnetization, *Journal of Geophysical Research*, B, Solid Earth and Planets, v. 96, no. 2, pp. 2007-2017.

Elmore, R.D., 2001, A review of palaeomagnetic dating on the timing and origin of multiple fluid-flow events in the Arbuckle Mountains, southern Oklahoma, *Petroleum Geoscience*, v. 7, pp. 223-229.

Elmore, R.D., Banerjee, S., Campbell, T., and Bixler, G., 1999, Paleomagnetic dating of ancient fluid-flow events and paleoplumbing in the Arbuckle Mountains, southern Oklahoma: In: Parnell, J., ed., *Dating and Duration of Fluid Flow Events and Rock-Fluid Interaction.* Geological Society, London, Special Publications, v. 144, pp. 9-25.

Elmore, R.D., London, D., Bagley, and Gao, G., 1993, Evidence for paleomagnetic dating of burial diagenesis by basinal fluids, Ordovician carbonates, Arbuckle Mountains, southern Oklahoma, *Applications of Paleomagnetism to Sedimentary Geology*, SEPM Special Publication, no. 49, pp. 115-128.

Enkin, R.J., Osadetz, K.G., Baker, J., and Kisilevsky, D., 2000, Orogenic remagnetizations in the Front Ranges and Inner Foothills of the southern Canadian Cordillera: Chemical harbinger and thermal handmaiden of Cordilleran deformation, *Geological Society of America Bulletin*, v. 112, no. 6, pp. 929-942.

Fisher, R.A., 1953, Dispersion on a sphere, *Proceedings of the Royal Society of London*, Series A, v. 217, pp. 295-305.

Fruit, D., Elmore, R.D., and Halgedahl, S., 1995, Remagnetization of the folded Belden Formation, *Journal of Geophysical Research*, v. 100, pp. 15,009-15,023.

Gao, G., Elmore, R.D., and Land, L.S., 1992, Geochemical constraints on the origin of calcite veins and associated limestone alteration, Ordovician Viola Group, Arbuckle Mountains, Oklahoma, U.S.A., *Chemical Geology*, v. 98, pp. 257-269.

Gill, J.D., Elmore, R.D., and Engel, M.H., 2002, Chemical remagnetization and clay diagenesis: testing the hypothesis in the Cretaceous sedimentary rocks of northwestern Montana, *Physics and Chemistry of the Earth*, v. 27, pp. 1131-1139.

Halgedahl, S.L. and Jarrard, R.D., 1995, Low-temperature behavior of single-domain through multidomain magnetite, *Earth and Planetary Science Letters*, v. 130, no. 1-4, pp. 127-139.

Heller, P.L., Bowdler, S.S., Chambers, H.P., Coogan, J.C., Hagen, E.S., Shuster, M.W., Winslow, N.S., and Lawton, T.F., 1986, Time of initial thrusting in the Sevier orogenic belt, Idaho-Wyoming and Utah, *Geology*, v. 14, no. 5, pp. 388-391.

Hirt, A.M., Banin, A., and Gehring, A.U., 1993, Thermal generation of ferromagnetic minerals from iron-enriched smectites, *Geophysical Journal International*, v. 115, no. 3, pp. 1161-1168.

Hudson, J.D., 1977, Stable isotopes and limestone lithification, *Journal of the Geological Society of London*, v. 133, pp. 637-660.

Huntoon, J.E., Hansley, P.L., and Naeser, N.D., 1999, The search for the source rock for the giant Tar Sand Triangle accumulation, southeastern Utah, *AAPG Bulletin*, v. 83, no. 3, pp. 467-495.

Jewell, P.W., Silberling, N.J., and Nichols, K.M., 2000, Geochemistry of the Mississippian Delle Phosphatic event, eastern Great Basin, U.S.A, *Journal of Sedimentary Research*, v. 70, no. 5, pp. 1222-1233.

Katz, B., Elmore, R.D., Cogoini, M., Engel, M.H., and Ferry, S., 2000, Associations between burial diagenesis of smectite, chemical remagnetization, and magnetite authigenesis in the Vocontian trough, SE France, *Journal of Geophysical Research*, v. 105, no. B1, pp. 851-868.

Keith, M.L., Weber, J.N., 1964. Carbon and oxygen isotopic compositions of selected limestone and fossils. *Geochimica et Cosmochimica Acta*, v. 28, pp. 1787-1816.

Kirschvink, J.L., 1980, The least-squares line and plane and the analysis of paleomagnetic data, *Geophysical Journal of the Royal Astronomical Society*, v. 62, no. 3, pp. 699-718.

Lewchuk, M.T., Elmore, R.D., and Evans, M., 2002, Remagnetization signature of Paleozoic sedimentary rocks from the Patterson Creek Mountain anticline in West Virginia, *Physics and Chemistry of the Earth*, v. 27, pp. 1141-1150.

Lowrie, W., 1990, Identification of ferromagnetic minerals in a rock by coercivity and unblocking temperature properties, *Geophysical Research Letters*, v. 17, no. 2, pp. 159-162.

McCabe, C., and Elmore, R.D., 1989, The occurrence and origin of late Paleozoic remagnetization in the sedimentary rocks of North America, *Reviews of Geophysics*, v. 27, pp. 471-494.

McCabe, C., Van der Voo, R., Peacor, D.R., Scotese, C.R., and Freeman, R., 1983, Diagenetic magnetite carries ancient yet secondary remanence in some Paleozoic sedimentary carbonates, *Geology*, v. 11, pp. 221-223.

McCrea, J.M., 1950, On the isotopic chemistry of carbonates and a paleothermometer scale, *Journal of Chemical Physics*, v. 18, no. 6, pp. 849-857.

McFadden, P.L., and Lowes, F.J., 1981, The discrimination of mean directions drawn from Fisher distributions, *Geophysical Journal of the Royal Astronomical Society*, v. 67, pp. 19-33.

Melker, Marc D., and Geissman, John W., 1997, Paleomagnetism of the Oquirrh Mountains and implications for the Cenozoic structural history of the easternmost Great Basin, in Geology and Ore Deposits of the Qquirrh and Wasatch Mountains, Utah, *Society of Economic Geologists Guidebook Series*, v. 29, pp. 91-112.

Morris, H.T. and Lovering, T.S., 1961, Stratigraphy of the east Tintic Mountains, Utah, *U.S. Geological Survey Professional Paper 361*, pp. 145.

Nichols, K.M., and Silberling, N.J., 1990, The Delle Phosphatic Member: an anomalous part of the Mississippian (Osagean-Meramecian) shelf sequence of central Utah, *Geology*, v. 18, pp. 46-49.

Nichols, K.M., and Silberling, N.J., 1993, Upper Devonian to Mississippian strata of the Antler foreland in the Leppy Hills, easternmost northern Nevada, *U.S. Geological Survey Bulletin*, 1988-G, pp. G1-G13.

Nichols, K.M., Silberling, N.J., and McCarley, L.A., 2002, Regional pattern of Mesozoic structures in the Confusion Range, westernmost central Utah, *Geological Society of America*, Denver Annual Meeting, Abstract.

Oliver, R., 1992, The spots and stains of plate tectonics, *Earth Science Reviews*, v. 32, pp. 77-106.

Pevear, D.R., 1999, Illite and hydocarbon exploration, *Proceedings of the National Academy of Sciences*, v. 96, no. 7, pp. 3440-3446.

Plaster-Kirk, L.E., Elmore, R.D., Engel, M.H. and Imbus, S.W., 1995, Paleomagnetic investigation of organic-rich lacustrine deposits, Middle Old Red Sandstone, Scotland, *Scottish Journal of Geology*, v. 32, no. 2, pp. 97-105.

Poole, F.G., and Claypool, G.E., 1984, Petroleum source-rock potential and crude-oil correlation in the Great Basin, *Hydrocarbon Source Rocks of the Greater Rocky Mountain Region*, Rocky Mountain Association of Geologists, pp. 179-230.

Pullaiah, G., Irving, E., Buchan, K.L., and Dunlop, D.J., 1975, Magnetization changes caused by burial and uplift, *Earth and Planetary Science Letters*, v. 28, pp. 133-143.

Sandberg, C.A., and Gutschick, R.C., 1980, Sedimentation and biostratigraphy of Osagean and Meramecian starved basin and foreslope, western United States, *Paleozoic Paleogeography of the West-Central U.S.*, Rocky Mountain Paleogeography Symposium 1, pp. 129-145.

Sandberg, C.A., and Gutschick, R.C., 1984, Distribution, microfauna, and source-rock potential of Mississippian Delle Phosphatic Member of Woodman Formation and equivalents, Utah and adjacent states, *Hydrocarbon Source Rocks of the Greater Rocky Mountain Region*, Rocky Mountain Association of Geologists, pp. 135-178.

Sandberg, C.A., Poole, F.G., and Gutschick, R.C., 1980, Devonian and Mississippian stratigraphy and conodont zonation of the Pilot and Chainman shales, Confusion Range, Utah, *Paleozoic Paleogeography of the West-Central U.S.*, Rocky Mountain Paleogeography Symposium 1, pp, 71-79.

Silberling, N.J., 2002, personal communication

Silberling, N.J., Trexler, J.H., Jr., Nichols, K.M., Jewell, P.W., and Crosbie, R.A., 1997, Overview of Mississippian depositional and paleotectonic history of the Antler foreland, eastern Nevada and western Utah, *Brigham Young University, Geology Studies*, v. 42, part I, pp. 161-197.

Stamatakos, J., Hirt, A.M., and Lowrie, W., 1996, The age and timing of folding in the central Appalachians from paleomagnetic results, *Geological Society of America Bulletin*, v. 108, no. 7, pp. 815-829.

Stueber, A.M., Pushkar, P., and Hetherington, E.A., 1984, A strontium isotopic study of Smackover brines and associated solids, southern Arkansas, *Geochimica et Cosmochimica Acta*, v. 48, pp. 1637-1649.

Swart, P.K., Burns, S.J., and Leder, J.J., 1991, Fractionation of the stable isotopes of oxygen and carbon in carbon dioxide during the reaction of calcite with phosphoric acid as a function of temperature and technique, *Chemical Geology*, v. 86, pp. 89-96.

Symons, D.T.A., and Cioppa, M.T., 2000, Crossover plots: A useful method for plotting SIRM data in paleomagnetism, *Geophysical Research Letters*, v. 27, pp.1779-1782.

Van der Voo, R., 1993, Paleomagnetics of the Atlantic, Tethys, and Iapetus oceans, Cambridge University Press.

Watson, G.S. and Enkin, R.J., 1993, The fold test in paleomagnetism as a parameter estimation problem, *Geophysical Research Letters*, v. 20, no. 19, pp. 2135-2137.

Weil, A.B. and Van der Voo, R., 2002, Insights into the mechanism for orogen-related carbonate remagnetization from growth of authigenic Fe-oxide: A scanning electron microscopy and rock magnetic study of Devonian carbonates from northern Spain, *Journal of Geophysical Research*, v. 107, no. B4, pp. 1-15.

Zijderveld, J.D.A., 1967, A.c. demagnetization of rocks: Analysis of results, *Methods in Paleomagnetism*, edited by D.E. Collinson, K.M. Creer and S.K. Runcorn, Elsevier, Amsterdam, pp. 254-286.

[redacted]